暗物质III

毕效军
中国科学院高能物理研究所

“2017 年理论物理前沿暑期讲习班——暗物质、
中微子与粒子物理前沿，
2017/7/26

看什么信号？Gamma，e+,pbar；什么实验探测？

看什么地方？暗物质信号，背景强度，天体环境等

$$\frac{dN}{dE} = \frac{\langle \sigma v \rangle}{2m_\chi^2} \sum_f B_f \frac{dN^f}{dE} \frac{\int \rho^2 dV}{4\pi d^2}$$

粒子物理模型；相互强度，末态？

Geometry of the propagation

Charged particles are confined within the propagation halo. It may contain particles propagated for a long time. To calculate the flux we have to solve a propagation equation.

the propagation geometry is like the figure, cosmic rays are confined within a larger cylinder with the height z ~ 4kpc, while the gas disk is only ~300pc.

But how to study the CR propagation??

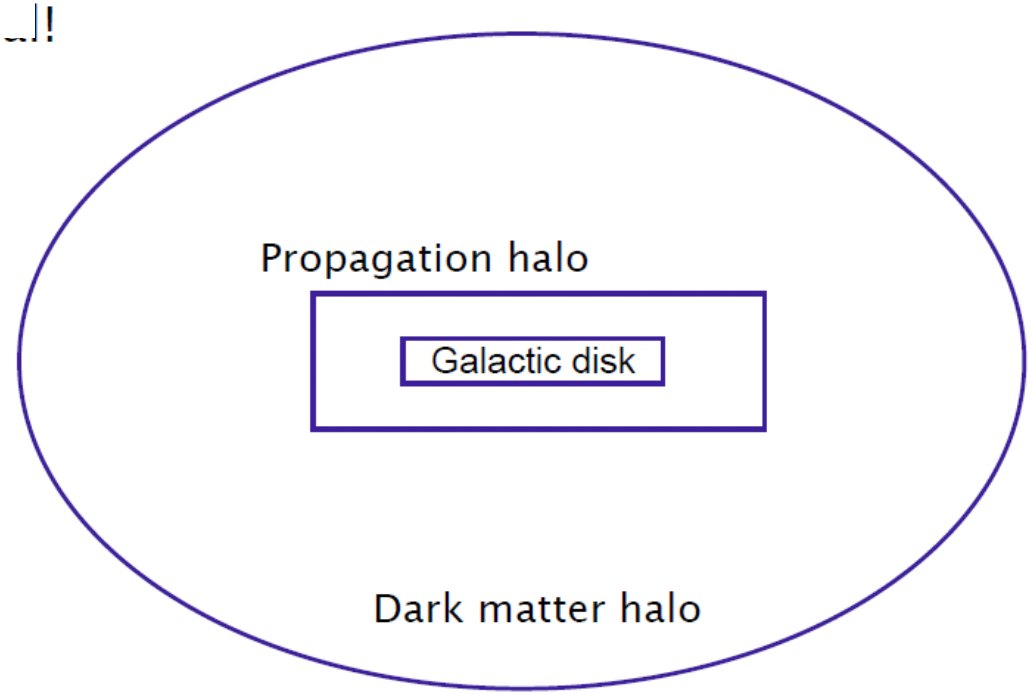

宇宙线的起源、加速

- 一般认为银河系宇宙线来自于超新星遗迹的加速

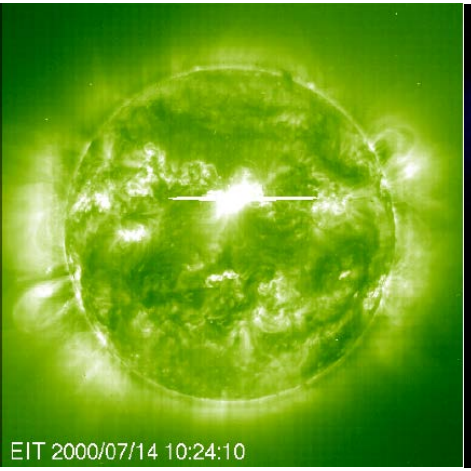

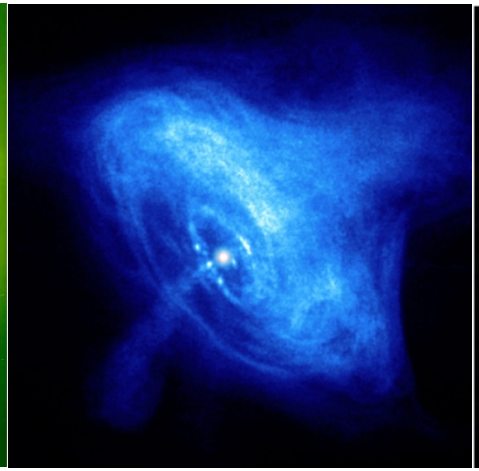

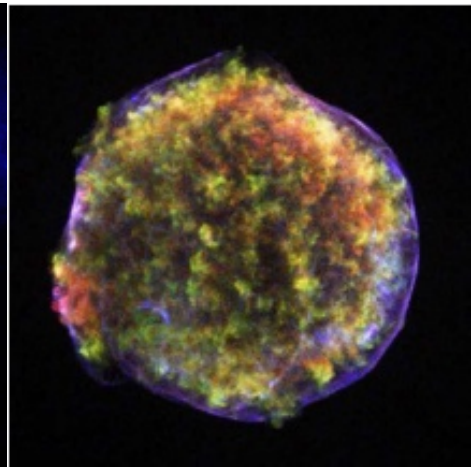

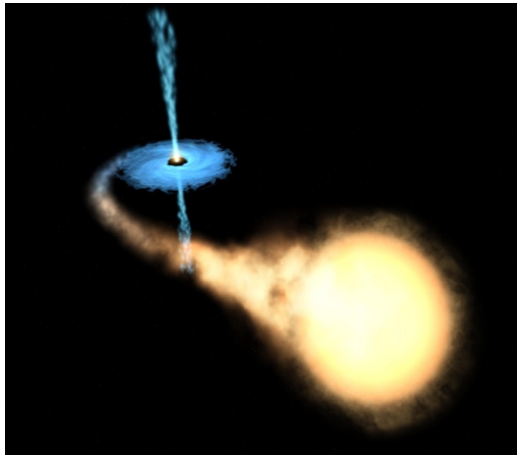

太阳（10^{11}eV）　　脉冲星，壳星超新星（$10^{14\text{-}16}$eV）　　微类星体，脉冲双星

Relative abundance of elements measured at CRs compared with the one in the solar system

- Both curves show the odd even effect, i.e. the tighter bound nuclei with an even numbers of protons and neutrons are more abundant.
- The main difference of the two curves is that the Li-Be-B group (Z = 3 − 5) and the Sc-Ti-V-Cr-Mn (Z = 21 − 25) group are much more abundant in cosmic rays than in the solar system.
- this is explained as the propagation effect, we will see later.

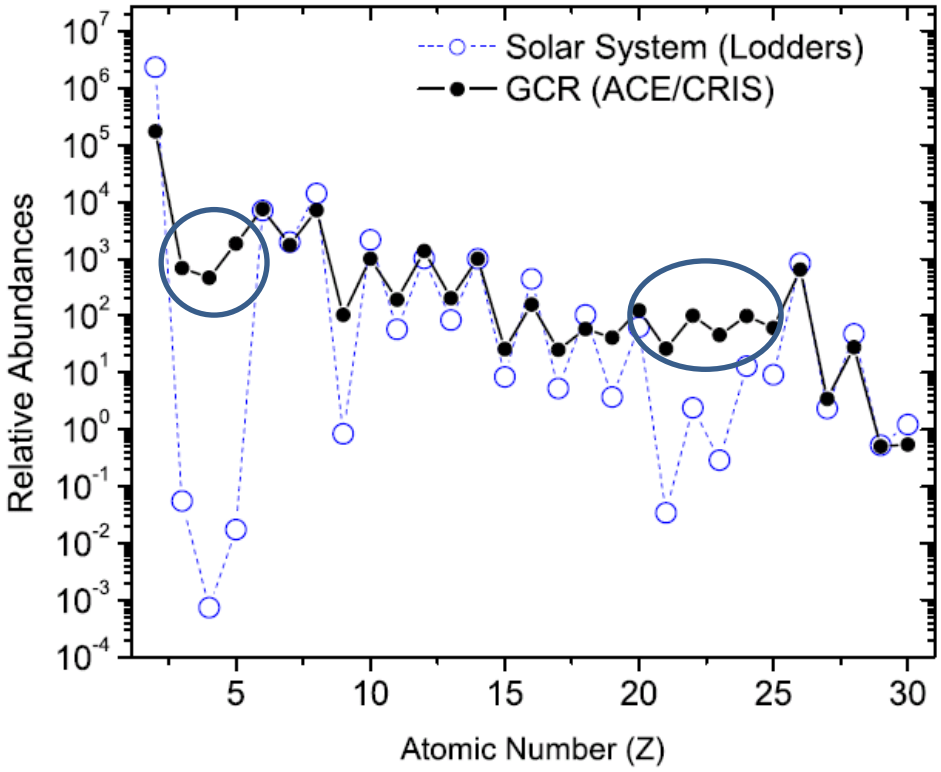

Propagation of cosmic rays

We want to explain the large over-abundance of the group Li-Be-B in cosmic rays compared to the Solar system by propagation effect. We consider two species, primaries with number density n_p and secondaries with number density n_s. If the two species are coupled by the spallation process p → s + X, then

$$\frac{\mathrm{d}n_p}{\mathrm{d}X} = -\frac{n_p}{\lambda_p},$$
$$\frac{\mathrm{d}n_s}{\mathrm{d}X} = -\frac{n_s}{\lambda_s} + \frac{p_{\mathrm{sp}} n_p}{\lambda_p}$$

where $X = \int \mathrm{d}l\, \rho(l)$ measures the amount of traversed matter, $\lambda_i = m/\sigma_i$ are the interaction lengths (in gr/cm2), and $p_{sp} = \sigma_{sp}/\sigma_{tot}$ is the spallation probability

The above equation is easily solved if using the initial condition ns(0) = 0

$$\frac{n_s}{n_p} = \frac{p_{\mathrm{sp}}\lambda_s}{\lambda_s - \lambda_p}\left[\exp\left(\frac{X}{\lambda_p} - \frac{X}{\lambda_s}\right) - 1\right]$$

If we consider as secondaries a group like Li-Be-B that has a much smaller abundance in the solar system than in cosmic rays, most of them have to be produced by spallation from heavier elements like the C-N-O group. With $\lambda_{CNO} \approx 6.7$ g/cm2, $\lambda_{LiBeB} \approx 10$ g/cm2, and $p_{sp} \approx 0.35$ measured at accelerators, the observed ratio 0.25 is reproduced for X ≈ 4.3 g/cm2,

Diffusion propagation

• With h = 300 pc ≈ 10^21 cm as thickness of the Galactic disc, $n_H \approx 1/cm^3$ as density of the interstellar medium, a cosmic ray following a straight line perpendicular the disc crosses only $X = m_H n_H h \approx 10^{-3} g/cm2$. The residence time of cosmic rays in the galaxy follows as $t \sim (4.3/10^{-3})(h/c) \sim 1.4 \times 10^{14} s \sim 5 \times 10^6$ yr. This result can only be explained, if the propagation of cosmic rays resembles a random-walk.

• considering the Lamor radius << h for cosmic rays with energy ~GeV – hundred TeV, random walk should be the realistic case.

The random walk can be described by the diffusion equation.

$$\frac{\partial n}{\partial t} - \nabla(D\nabla n) = Q$$

D is the diffusion coefficient, Q is the source term.

The Green's function of this equation is

$$G(r) = \frac{1}{(4\pi Dt)^{3/2}} \exp[-r^2/(4Dt)]$$

Then we get the traveled distance is ~ $\sqrt{Dt}$. For random walk $\langle r^2 \rangle \sim N l_0^2$ ~Dt, we have $D = l_0 v/3$, mean l_0 is the mean free path

完整的宇宙线传播方程

- 需要了解宇宙线中的原子核、正负电子、伽玛光子和同步辐射
- 利用真实的天体物理信息，如银河系结构、星际气体、星际辐射场和磁场的分布等
- 包括各种相互作用过程，以及宇宙线传播的各种效应

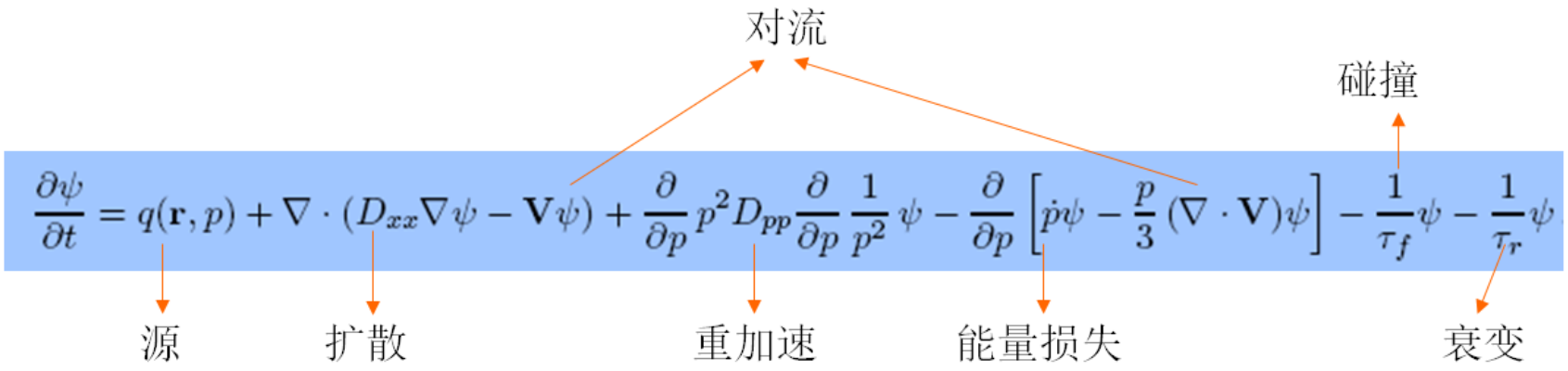

银河系宇宙线的传播

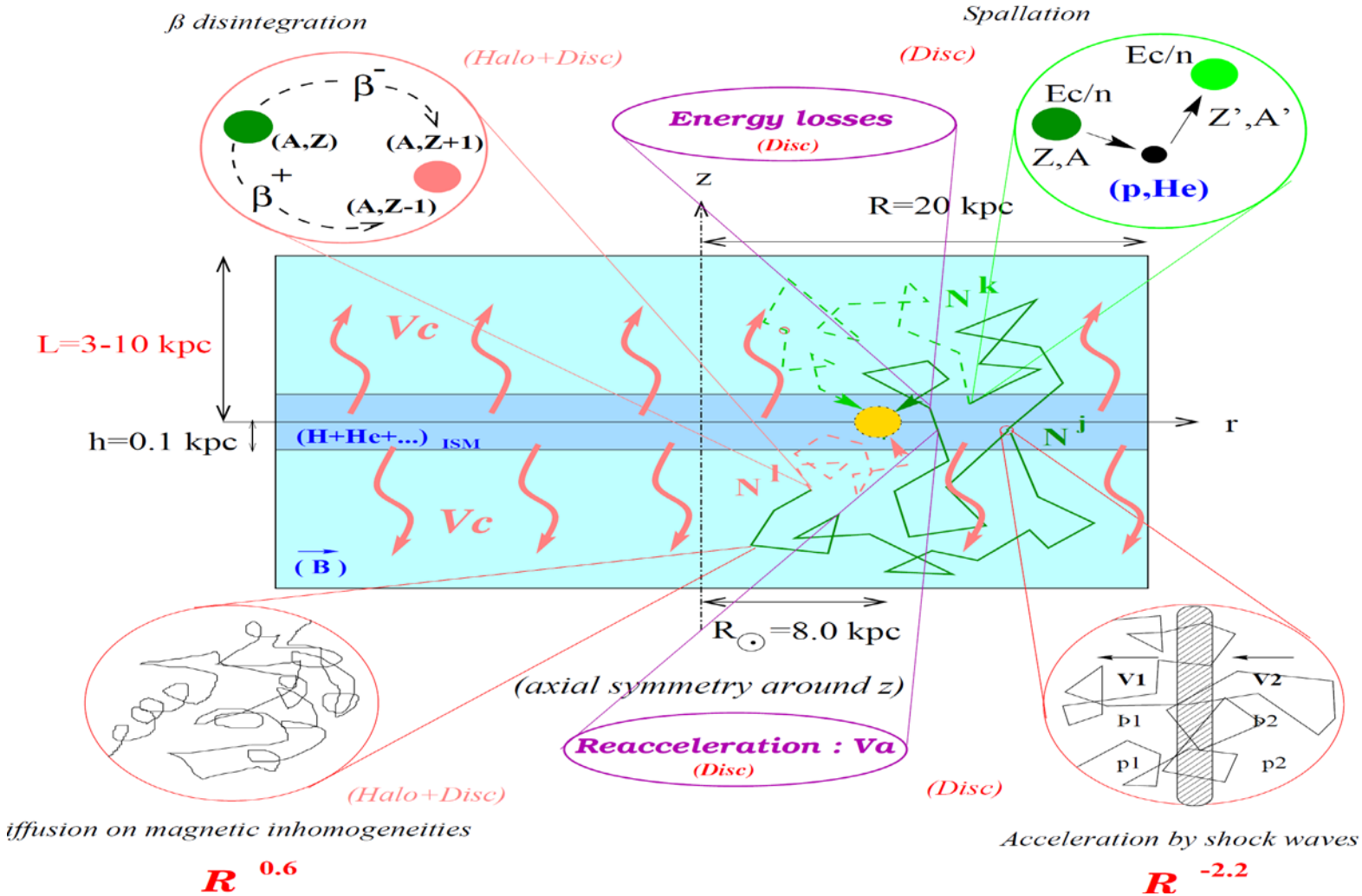
ß disintegration
(Halo+Disc)
Spallation
(Disc)
Energy losses
(Disc)
Ec/n
Ec/n
Z',A'
Z,A
(p,He)
β⁻
(A,Z)
(A,Z+1)
β⁺
(A,Z-1)
z
R=20 kpc
L=3-10 kpc
h=0.1 kpc
Vc
Vc
(H+Hc+...) ISM
(B)
r
N k
N j
N i
R⊙=8.0 kpc
(axial symmetry around z)
Reacceleration : Va
(Disc)
(Halo+Disc)
(Disc)
V1
V2
p1
p2
p1
p2
iffusion on magnetic inhomogeneities
R 0.6
Acceleration by shock waves
R -2.2

银河系宇宙线的传播

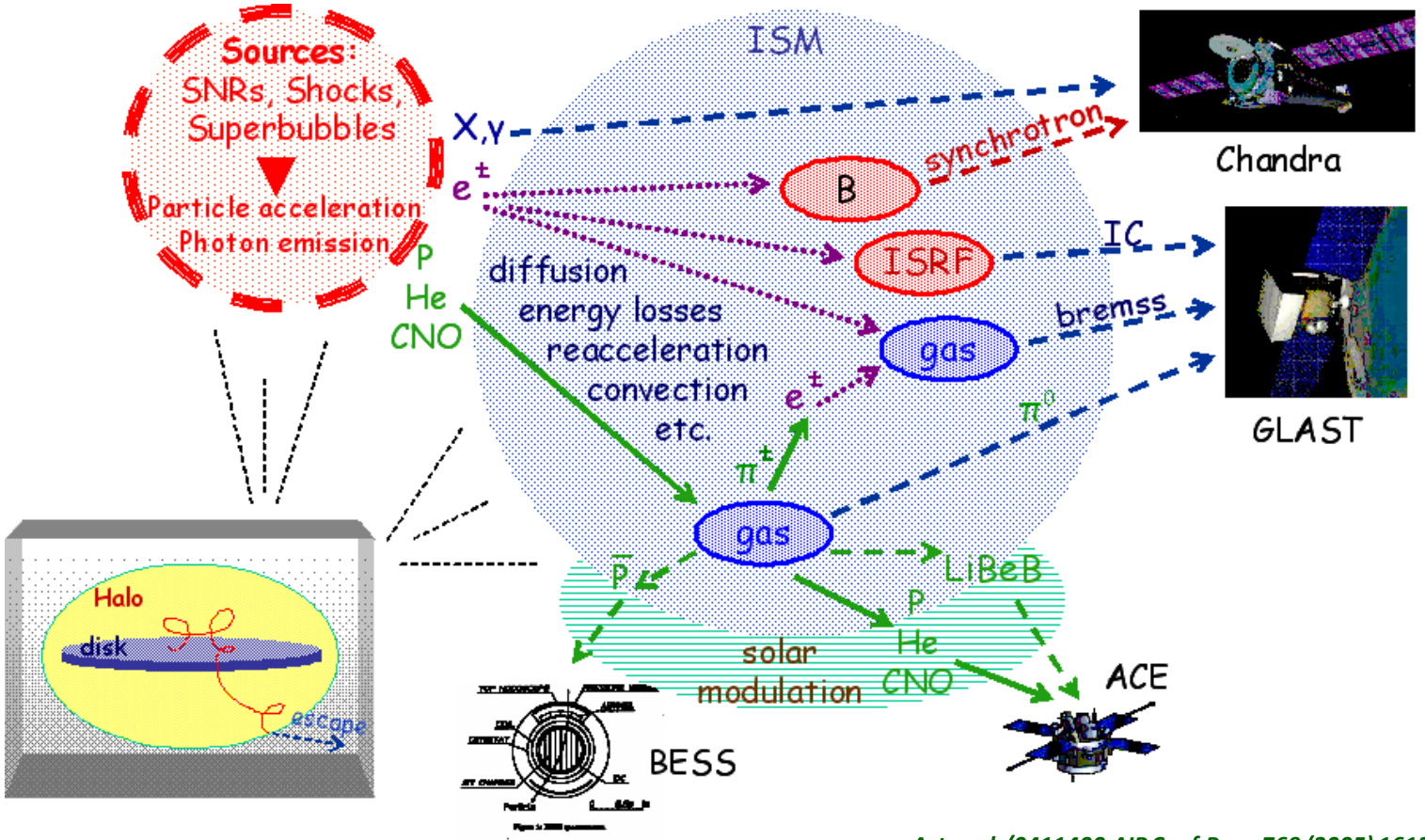

Astro-ph/0411400,AIP Conf.Proc. 769 (2005) 1612-1617

B/C determines the diffusion coefficient

- In order to explain the B/C data, the higher energy has less B/C with a power law， it requires that $D \propto E^{\alpha}$

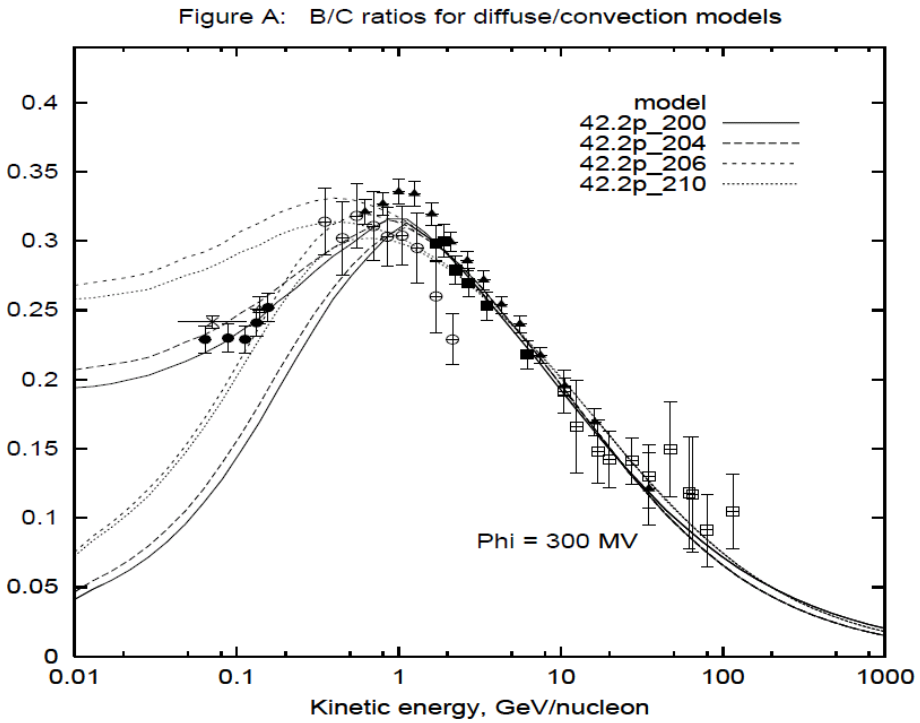

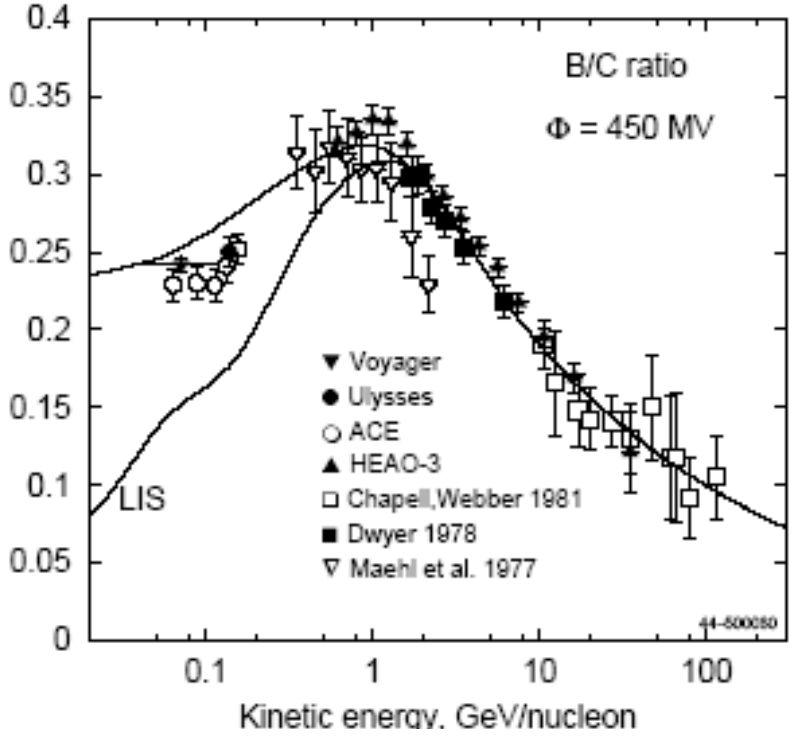

Sec/prim 将敏感地依赖于传播模型，所以常被用于决定模型参量．B/C 是目前测量得最多最好的．

传播参数

宇宙线粒子传播

γ 射线

反物质

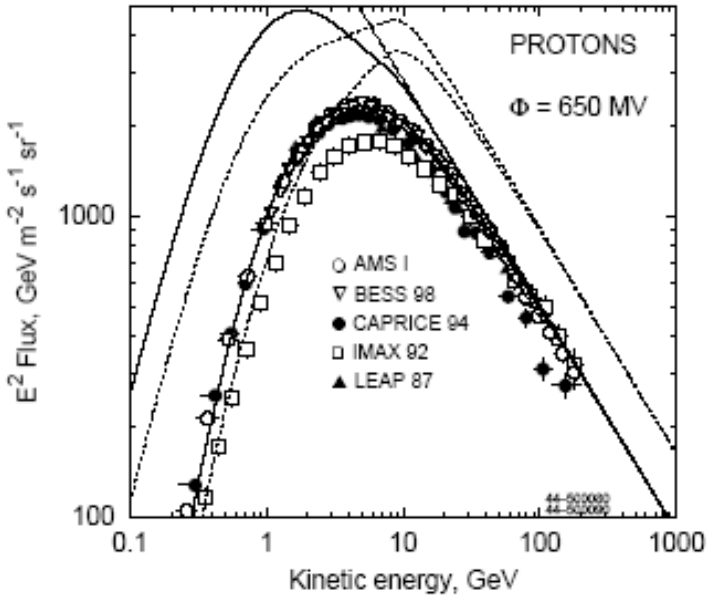

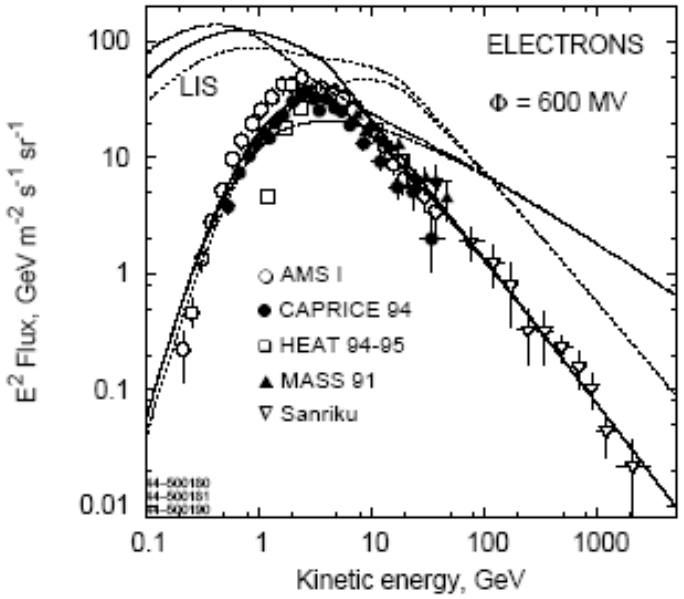

Galactic diffuse gamma-rays

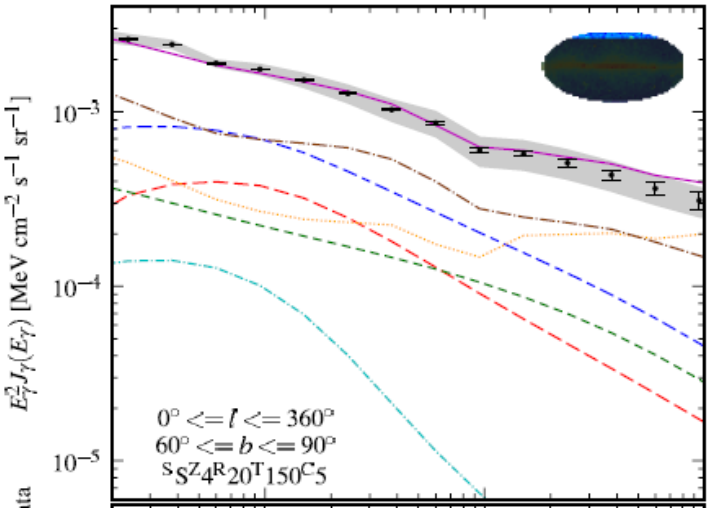

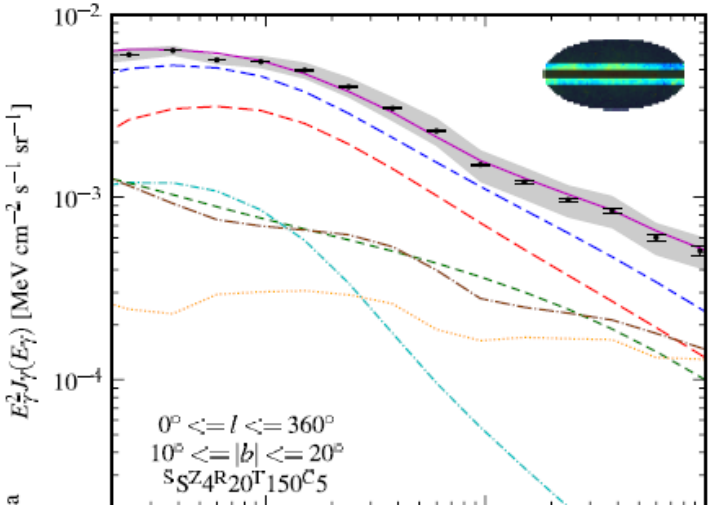

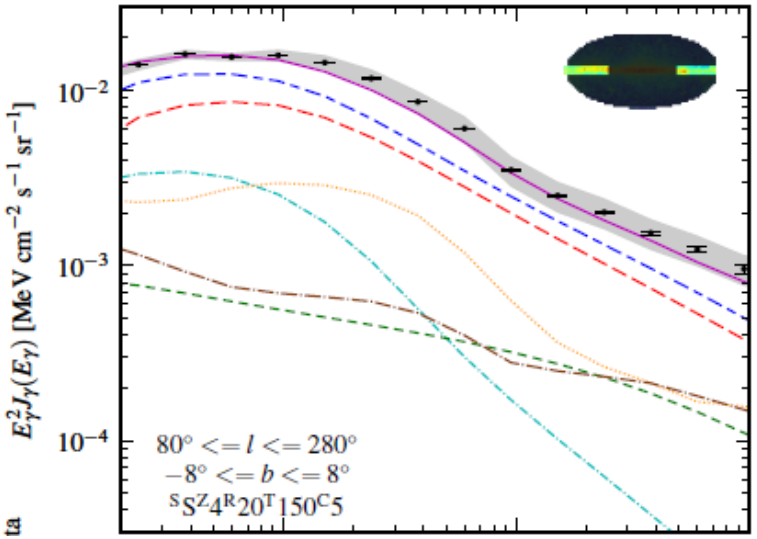

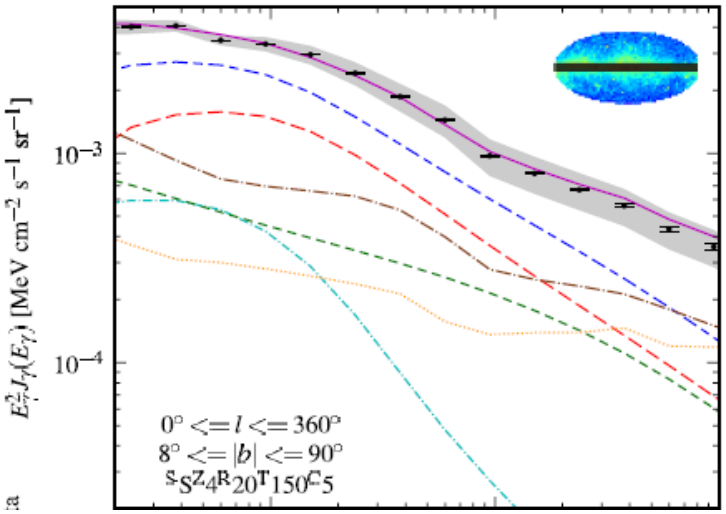

Anti-proton ratio

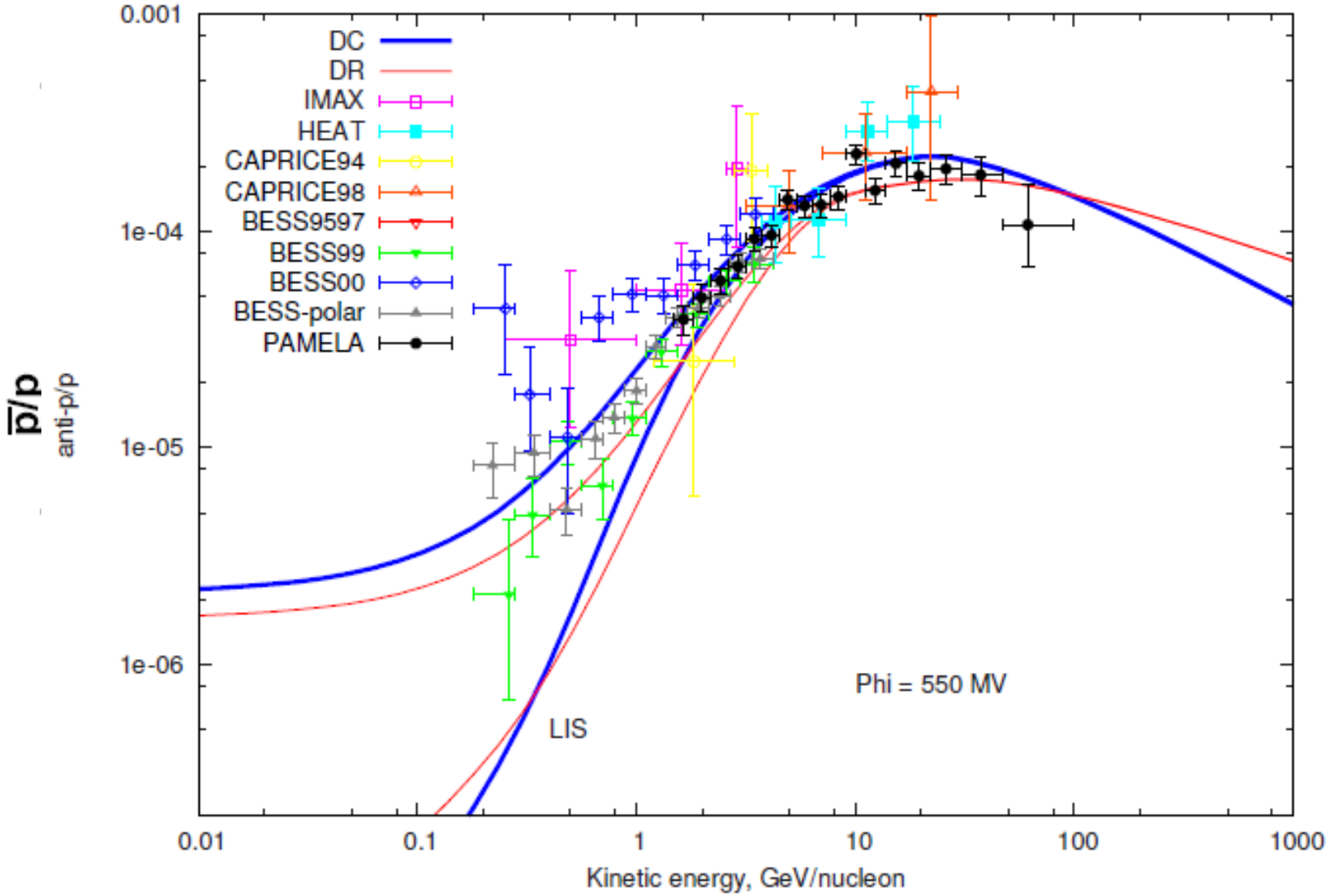

基于AMS02最新数据的传播研究

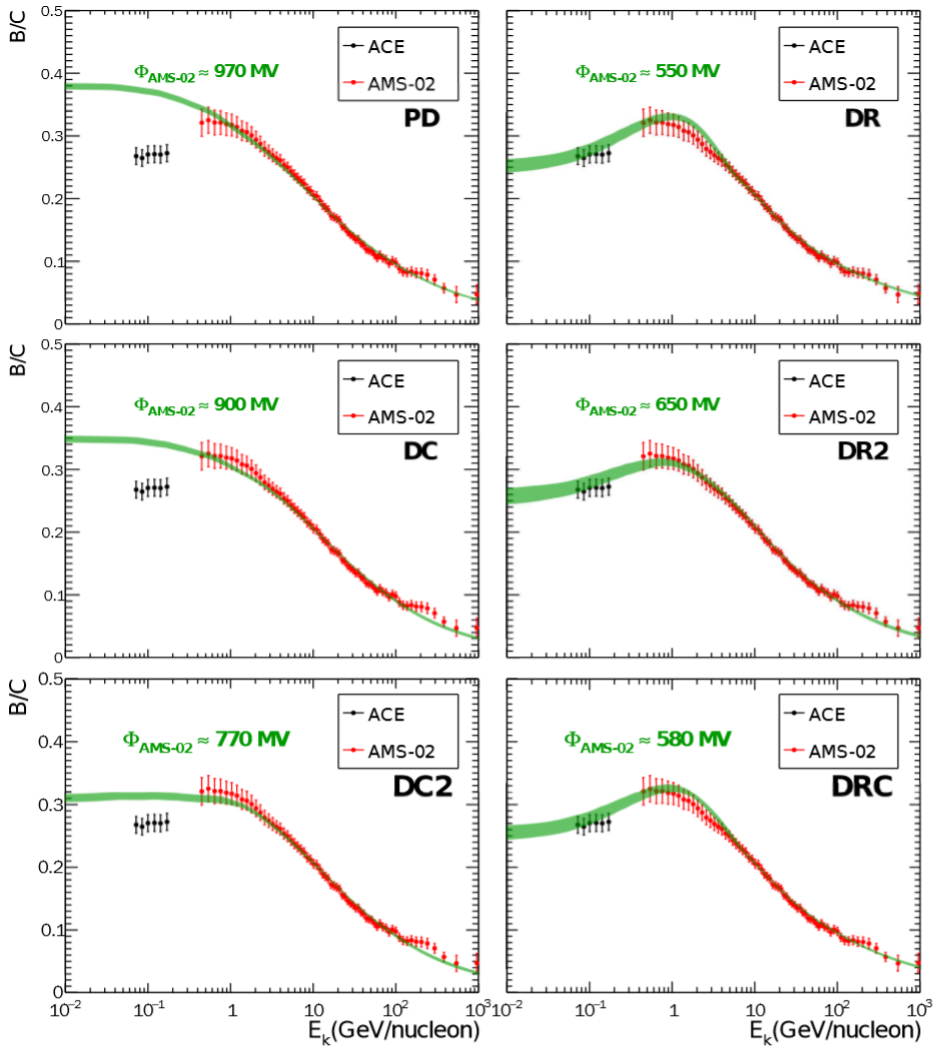

基于AMS02最新数据的传播研究

TABLE II: Posterior mean and 68% credible uncertainties of the model parameters

	Unit	PD	DC	DC2	DR	DR2	DRC
D_0	$(10^{28}\mathrm{cm^2 s^{-1}})$	5.29 ± 0.51	4.20 ± 0.30	4.95 ± 0.35	7.24 ± 0.97	4.16 ± 0.57	6.14 ± 0.45
δ		0.471 ± 0.006	0.588 ± 0.013	0.591 ± 0.011	0.380 ± 0.007	0.500 ± 0.012	0.478 ± 0.013
z_h	(kpc)	6.61 ± 0.98	10.90 ± 1.60	10.80 ± 1.30	5.93 ± 1.13	5.02 ± 0.86	12.70 ± 1.40
v_A	$(\mathrm{km\,s^{-1}})$	—	—	—	38.5 ± 1.3	18.4 ± 2.0	43.2 ± 1.2
dV_c/dz	$(\mathrm{km\,s^{-1}\,kpc^{-1}})$	—	5.36 ± 0.64	5.02 ± 0.55	—	—	11.99 ± 1.26
R_0	(GV)	—	—	5.29 ± 0.23	—	—	—
η		—	—	—	—	-1.28 ± 0.22	—
$\log(A_p)^a$		-8.334 ± 0.003	-8.334 ± 0.003	-8.336 ± 0.003	-8.347 ± 0.002	-8.334 ± 0.002	-8.345 ± 0.002
ν_1		2.44 ± 0.01	2.45 ± 0.01	2.43 ± 0.01	1.69 ± 0.02	2.04 ± 0.03	1.82 ± 0.02
ν_2		2.34 ± 0.03	2.30 ± 0.01	2.30 ± 0.01	2.37 ± 0.01	2.33 ± 0.01	2.37 ± 0.01
$\log(R_{br})^b$		5.06 ± 0.13	4.82 ± 0.05	4.78 ± 0.06	4.11 ± 0.02	4.03 ± 0.03	4.22 ± 0.03
Φ_0	(MV)	0.595 ± 0.005	0.537 ± 0.006	0.419 ± 0.005	0.180 ± 0.008	0.290 ± 0.014	0.220 ± 0.008
Φ_1	(MV)	0.495 ± 0.011	0.485 ± 0.011	0.472 ± 0.012	0.487 ± 0.011	0.485 ± 0.011	0.482 ± 0.013
χ^2/dof		748.6/463	591.0/462	494.6/461	438.8/462	341.0/461	380.5/461

[a] Propagated flux normalization at 100 GeV in unit of $\mathrm{cm^{-2}s^{-1}sr^{-1}MeV^{-1}}$

[b] Break rigidity of proton injection spectrum in unit of MV

Propagation of electron/positrons

- For electrons, spallation is irrelevant.
- above a few GeV the reacceleration and convection are not so important
- Diffusion of electron/positrons are given by

$$\partial_t \mathcal{N} - \boldsymbol{\nabla} \cdot \{K(E) \boldsymbol{\nabla} \mathcal{N}\} + \partial_E \left\{ \frac{dE}{dt} \mathcal{N} \right\} = \mathcal{Q}(E, \boldsymbol{x}, t)$$

- Only the energy loss term is considered as others are neglected.

Green's function method

- Assuming that spatial diffusion and energy losses are isotropic and homogeneous, it is easy to derive the steady state Green's function in an infinite 3D space, we get

$$\widehat{\mathcal{D}}_{\bar{t}}\,\mathcal{G} = \delta^3(\boldsymbol{x}-\boldsymbol{x}_s)\delta(E-E_s),\ i.e.,$$

$$\mathcal{G}(\boldsymbol{x}, E \leftarrow \boldsymbol{x}_s, E_s) = \frac{1}{b(E)\,(\pi\,\lambda^2)^{\frac{3}{2}}} \cdot \exp\left\{-\frac{(\boldsymbol{x}_s-\boldsymbol{x})^2}{\lambda^2}\right\}$$

- the subscript s represents quantities at source
- We define the energy-loss rate and the diffusion scale to be

$$b(E) \equiv -\frac{dE}{dt}\ ;\quad \lambda^2 \equiv 4\int_E^{E_s} dE'\,\frac{K(E')}{b(E')}$$

Boundary conditions

- To give vertical boundary condition, one can split the general Green's function into two terms, one radial and the other vertical, as
- $$\mathcal{G} = (\mathcal{G}_r \times \mathcal{G}_z)/b(E)$$
- The radial term is just the infinite 2D solution

$$\mathcal{G}_r(\boldsymbol{r}, E \leftarrow \boldsymbol{r}_s, E_s) = \frac{1}{\pi\,\lambda^2} \exp\left\{-\frac{(\boldsymbol{r}-\boldsymbol{r}_s)^2}{\lambda^2}\right\}$$

- For vertical solution it is divided by two cases, that the propagation scale is small $\lambda < L,$ or large

- For $\lambda < L$, a solution like the charge image method gives (Baltz & Edsjo ̈ 1998)

$$\mathcal{G}_z(z, E \leftarrow z_s, E_s) = \sum_{n=-\infty}^{+\infty} \frac{(-1)^n}{\sqrt{\pi}\lambda} \exp\left\{-\frac{(z - z_{s,n})^2}{\lambda^2}\right\}$$

- where $z_{s,n} \equiv 2nL + (-1)^n z_s$
- For large scale $\lambda \gtrsim L$ a better solution gives faster convergence (Lavalle et al. 2007)

$$\mathcal{G}_z(z, E \leftarrow z_s, E_s) = \frac{1}{L} \sum_{n=1}^{+\infty} \left\{ e^{-\left[\frac{k_n \lambda}{2}\right]^2} \phi_n(z)\phi_n(z_s) \right.$$

- $$\left. + e^{-\left[\frac{k'_n \lambda}{2}\right]^2} \phi'_n(z)\phi'_n(z_s) \right\},$$

- Where

$$k_n = (n - 1/2)\pi/L \quad ; \quad k'_n = n\pi/L \, ;$$
$$\phi_n(z) = \sin\left(k_n(L - |z|)\right) \quad ; \quad \phi'_n(z) = \sin\left(k'_n(L - z)\right)$$

Time dependent solution

- The steady-state solutions derived above are very good approximations for a continuous injection of CRs in the ISM, such as for the secondaries.
- In opposition, primary CRs are released at localized events, such as supernova remnants and sometimes pulsars. They are generally assumed the most common Galactic CR accelerators
- Since electrons lose energy very fast, there is a spatial scale (an energy scale, equivalently), below (above energy) which these local variations will have a significant effect on the local electron density.
- For $\Gamma_\star(\lambda/R)^2 \gg b(E)/E.$ for D ~ 0.01kpc^2/Myr, R = 20kpc
- $$b(E) \approx (\mathrm{GeV/Myr}/315)\epsilon^2 \text{ and } \Gamma_\star \approx 1/100\,\mathrm{yr},$$
- It is found that only for E ~< 80GeV, the electron/positron flux is smooth without large fluctuation.

Time dependent solution

- To estimate the contribution of local transient sources, we need to solve the full time-dependent transport equation. We will show that the method used for the steady-state case is still useful
- We need to solve the Green's function of

$$\widehat{\mathcal{D}}\,\mathcal{G}_t \;=\; \delta^3(\boldsymbol{x}-\boldsymbol{x}_s)\delta(E-E_s)\delta(t-t_s)$$

- we generally work in Fourier space (Baltz & Wai 2004)

$$\mathcal{G}_t(t,E,\boldsymbol{x}) \;=\; \frac{1}{(2\pi)^2}\iint d^3k\,d\omega$$

$$\times\exp\left\{i\big(\boldsymbol{k}\cdot\boldsymbol{x}+\omega t\big)\right\}\;\phi(\omega,E,k)$$

Time dependent Green's function

- In Fourier space, we derive the ordinary differential equation for E

$$\left\{i\omega + k^2 K(E)\right\}\phi - \partial_E\Big(b(E)\phi\Big) = \delta(E - E_s) \qquad (1$$
$$\times \frac{1}{(2\pi)^2}\exp\left\{-i(\boldsymbol{k}\cdot\boldsymbol{x}_s + \omega t_s)\right\}$$

- With soluton

$$\phi(\omega, E, k) = \frac{1}{b(E)}\frac{1}{(2\pi)^2}\exp\left\{-\frac{1}{4}k^2\lambda^2 - i\boldsymbol{k}\cdot\boldsymbol{x}_s\right\}$$
$$\times \exp\left\{-i\omega(t_s + \Delta\tau)\right\}\ .$$

Time dependent Green's function

- The inverse Fourier transformation is straightforward and eventually we have

$$\mathcal{G}_t(t, E, \boldsymbol{x} \leftarrow t_s, E_s, \boldsymbol{x}_s) = \frac{\delta(\Delta t - \Delta\tau)}{b(E)} \frac{\exp\left\{-\frac{(\boldsymbol{x}-\boldsymbol{x}_s)^2}{\lambda^2}\right\}}{(\pi\lambda^2)^{3/2}}$$

- where $\Delta t = t - t_s$ and $\Delta\tau(E, E_s) \equiv \int_E^{E_s} \frac{dE'}{b(E')}$

- We recognize the product of the steady state solution and a delta function of the real time and loss time for energy from Es to E

- $$\mathcal{G}_t(t, E, \boldsymbol{x} \leftarrow t_s, E_s, \boldsymbol{x}_s) = \delta(\Delta t - \Delta\tau)\, \mathcal{G}(E, \boldsymbol{x} \leftarrow E_s, \boldsymbol{x}_s)$$

Approximated links between propagation models and observed spectra

- The energy dependence in the electron propagation comes from spatial diffusion and energy losses.
- At high energy, one can assume that the propagation scale is short enough to allow us to neglect the vertical boundary condition
- we assume that a source term that is homogeneously distributed in the disk. This is a very good approximation for secondaries and fair enough for primaries.
- The source term can be approximately given
- $$\mathcal{Q}(E, \boldsymbol{x}) = 2\, h^{'}\, ^{'} \mathcal{Q}_0\, \delta(z)\, \epsilon^{-\gamma}$$

Power-law index value

- Then we derive the propagated flux at the position of the solar system as

$$\phi_{\odot}(E) \simeq \frac{o\,c\,h}{2\,\pi^{3/2}} \frac{\mathcal{Q}_0}{\sqrt{K_0/\tau_l}} \epsilon^{-\widetilde{\gamma}}$$

- Where $o = \sqrt{\alpha - \delta - 1}/(\gamma - 1) = \mathcal{O}(1)$,
- especially we have

$$\widetilde{\gamma} = \gamma + \frac{1}{2}(\alpha + \delta - 1)$$

- Where γ, α, δ are power-law indices of source, energy loss and propagation parameter.

Injection index

- the energy-loss rate is dominated by inverse Compton and synchrotron processes. In the nonrelativistic Thomson approximation, we have α=2. then we have $\widetilde{\gamma} = \gamma + \frac{1}{2}(1+\delta)$
- For the observed $\widetilde{\gamma} \approx 3$ we have γ=[2.1,2.35] for $\delta \in [0.3, 0.8]$.
- Although it is a very useful approximation at first order, this analysis is valid only for a smooth and flat distribution of sources. For a local discrete source the local effects have to be taken into account

Point sources

- For a single event-like source, which will differ from the above calculation,

$$\mathcal{Q}_\star = Q_{\star,0}\delta(|\boldsymbol{x}_s| - d)\,\delta(t_s - t_\star)\,\epsilon^{-\gamma}$$

- We assume the source is located within the propagation length $d \ll \lambda$ and the source is a burst at a time much earlier than the energy-loss timescale $t_\star \ll \tau_l$. we then get

$$\phi_\odot(E) = \frac{\beta\, c}{4\pi}\,\frac{b(E^\star)}{b(E)}\,\frac{Q_{\star,0}\,\epsilon_\star^{-\gamma}}{(\pi\lambda^2)^{3/2}} \simeq \frac{c}{4\pi}\,\frac{Q_{\star,0}\,\epsilon^{-\widetilde{\gamma}_\star}}{(4\,\pi\,K_0\,t_\star)^{3/2}}$$

- With $\widetilde{\gamma}_\star = \gamma + \frac{3}{2}\delta$;
- we notice that γ is larger and the index is independent of the energy loss as $t_\star \ll \tau_l$

Secondaries

- the steady-state source term for secondaries cans be written as

$$\mathcal{Q}_s(E, \boldsymbol{x}) = 4\pi \sum_{i,j} \int dE' \, \phi_i(E', \boldsymbol{x}) \, \frac{d\sigma_{ij}(E', E)}{dE} \, n_j(\boldsymbol{x})$$

- where i represents the CR species of the flux ϕ and j the ISM gas species of density n, the latter being concentrated within the thin Galactic disk, and $d\sigma_{ij}(E',E)$ is the inclusive cross section for a CR-atom interaction to produce an electron or positron at energy E.

Secondary electron/positron

- The calculated flux of secondary electrons and positrons are
- Numerical

calculation of spectrum is needed

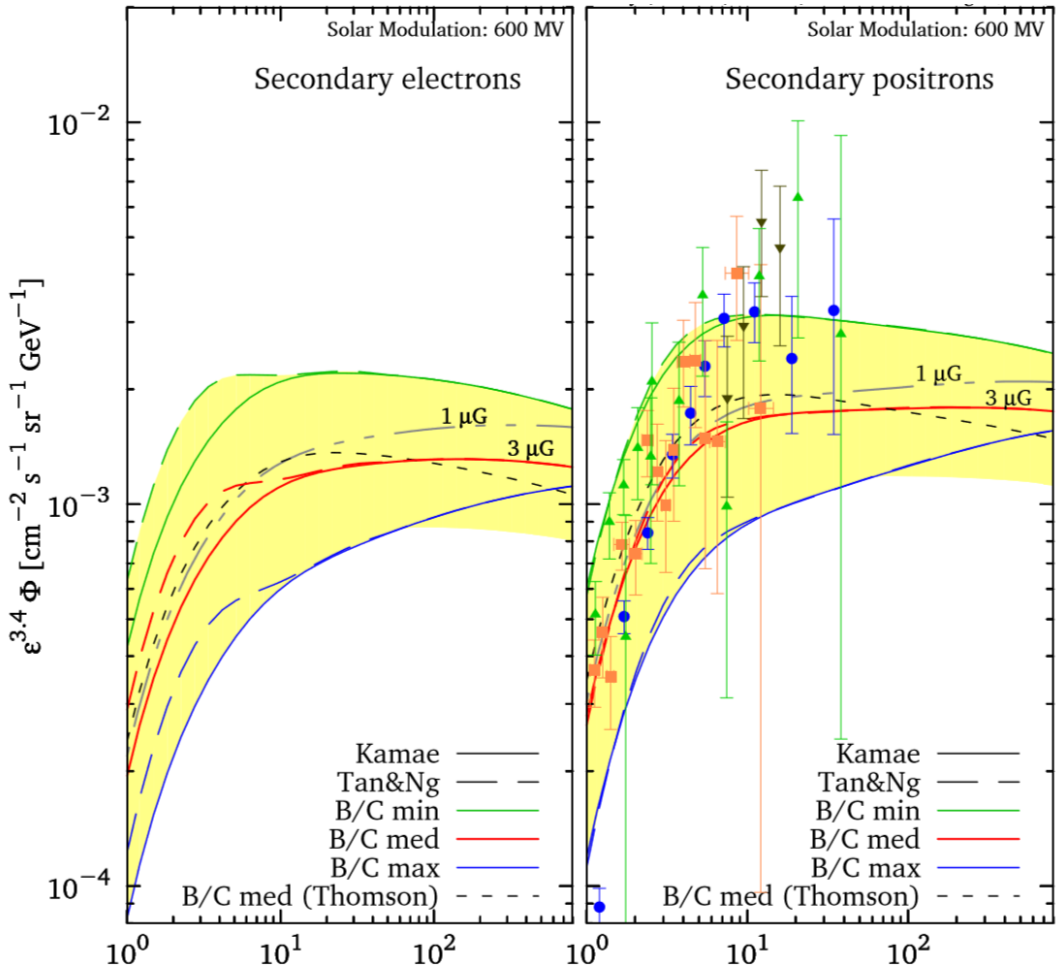

Uncertainties of point sources propagation

- The theoretical errors for the observed spectrum calculation originate from uncertainties (i) in the spectral shape and normalization at the source, (ii) the distance estimate, (iii) the age estimate and (iv) propagation uncertainties.

Discussion of the uncertainties for a single source spectrum

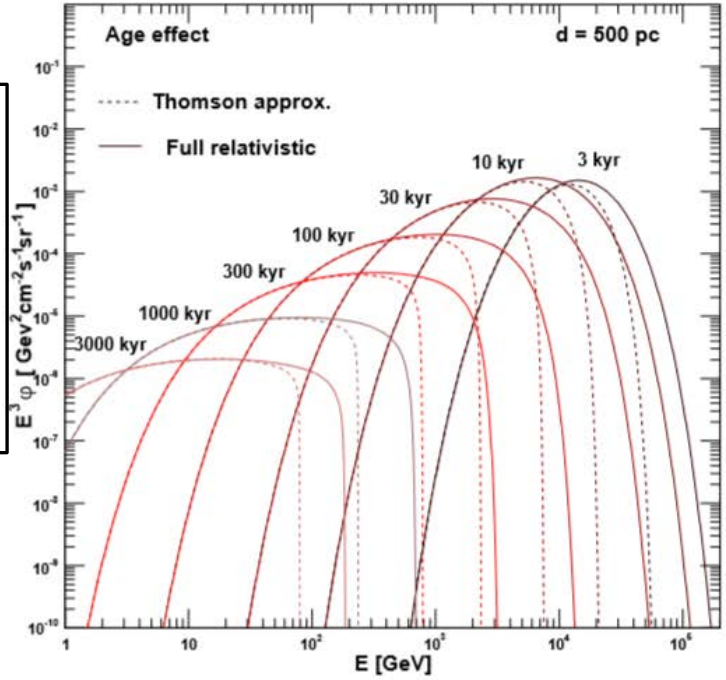

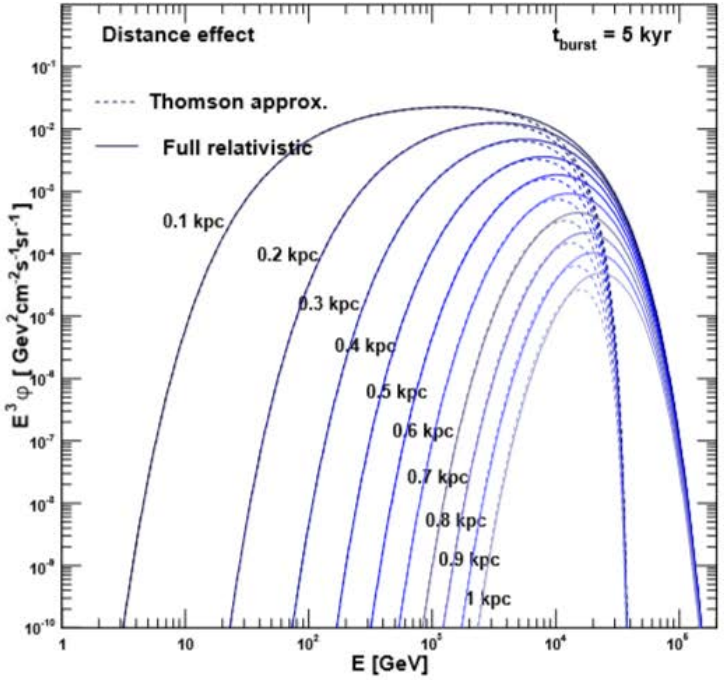

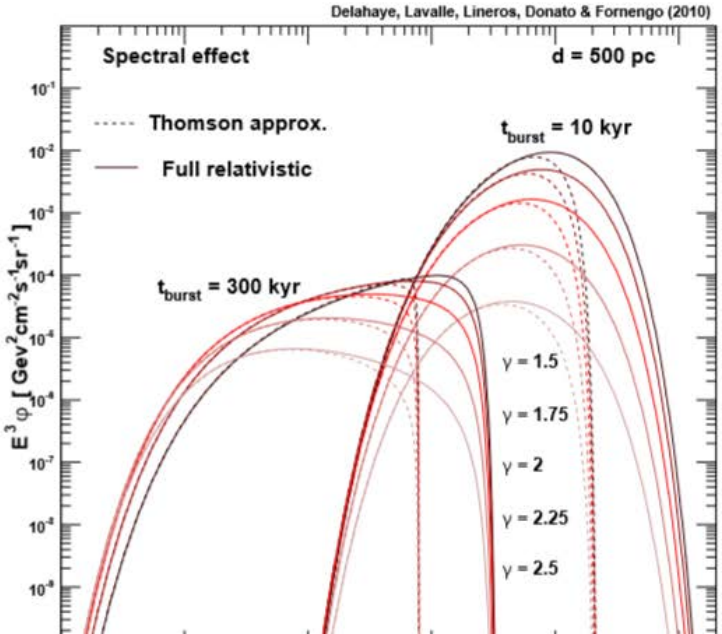

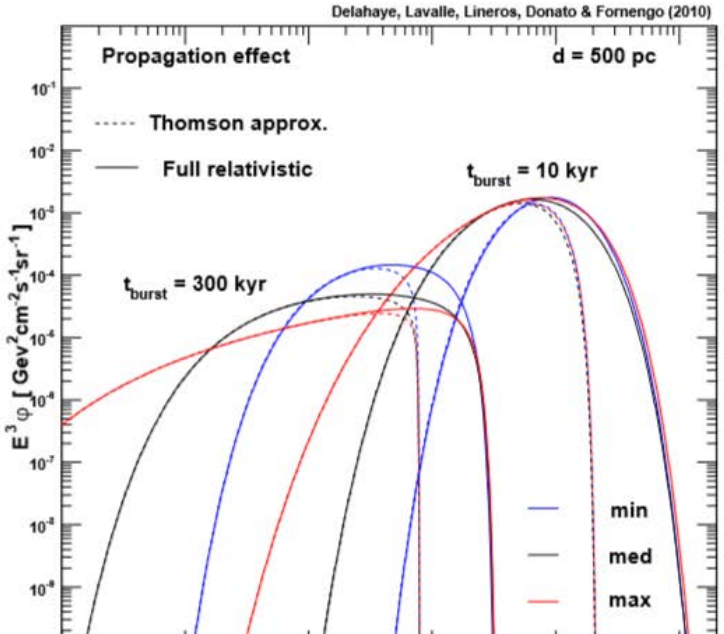

Electrons from some local SNRs

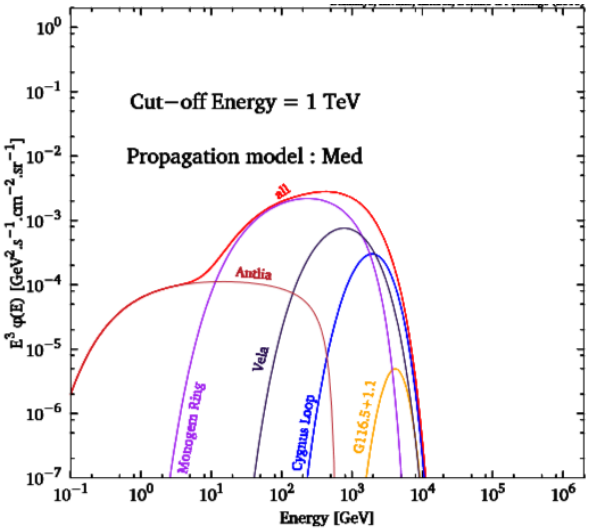

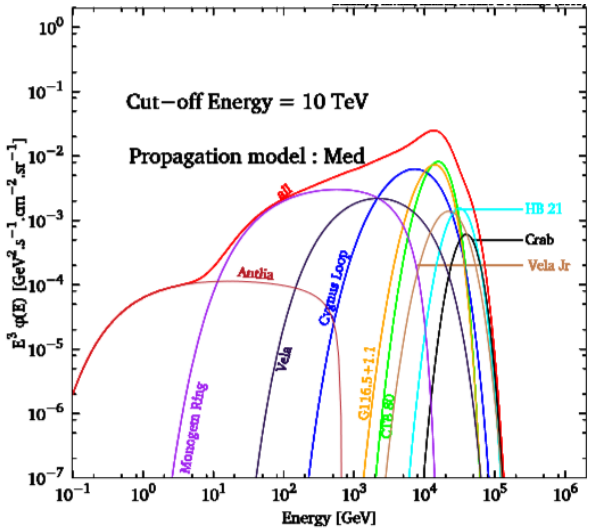

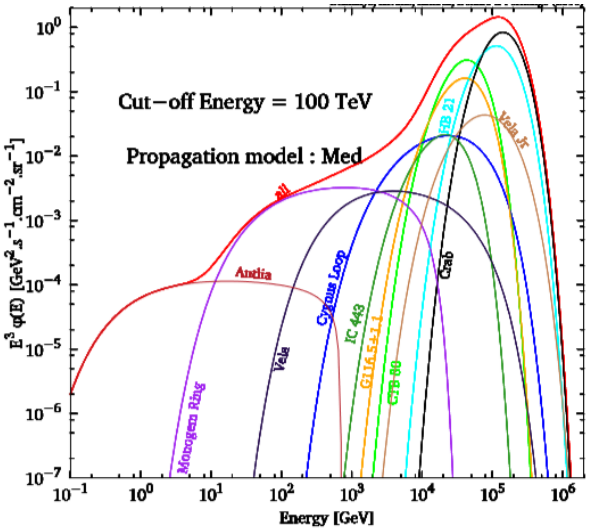

AMS02是国际空间站上唯一大型科学实验，将长期在轨运

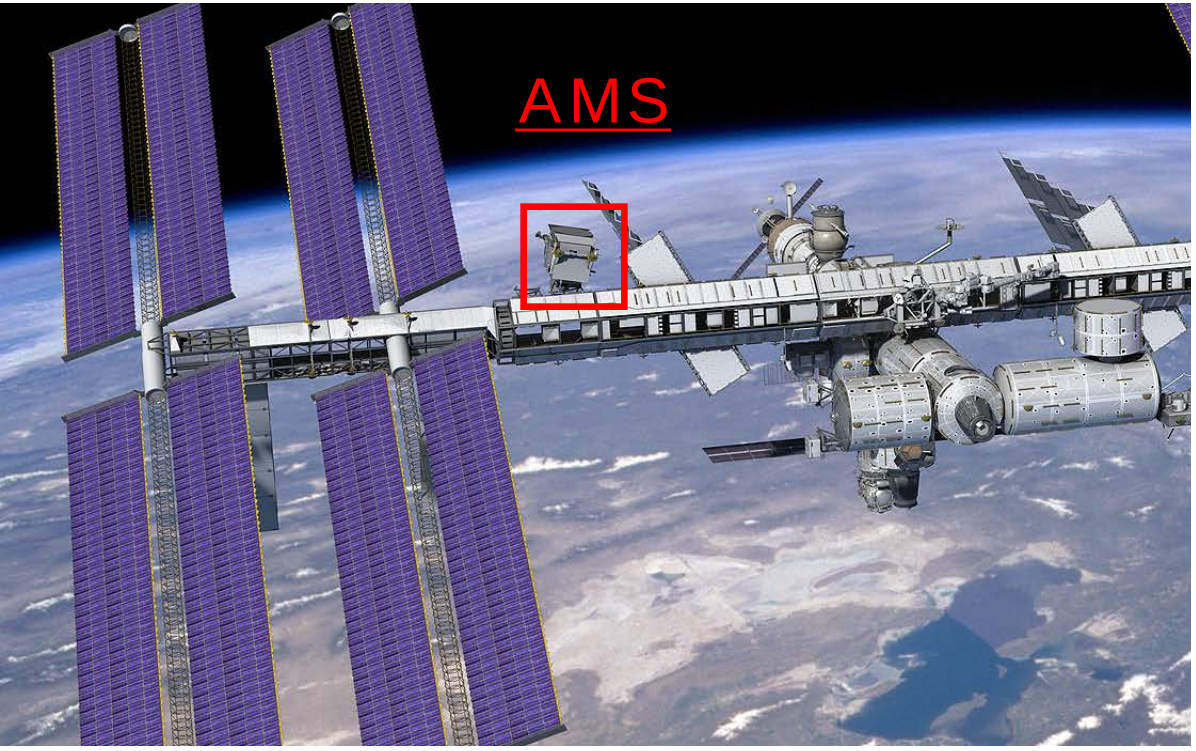

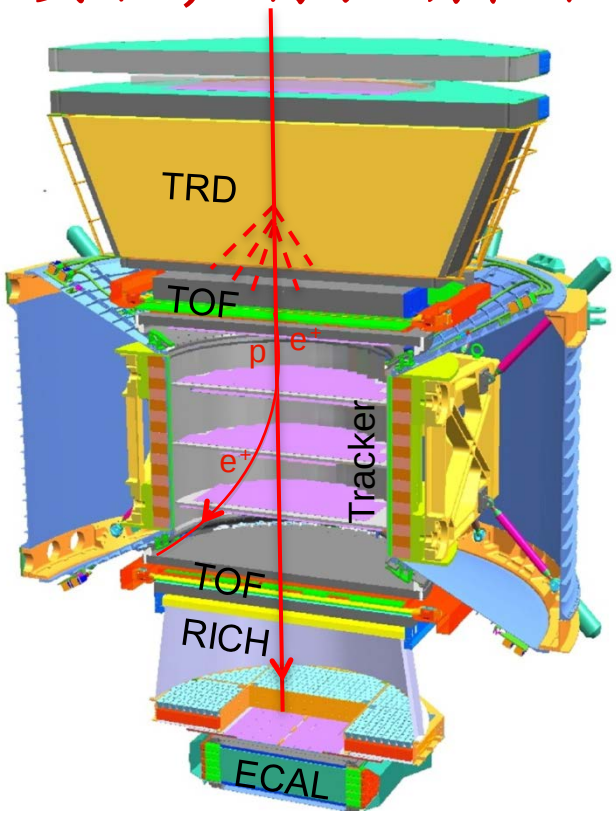

AMS物理目标：暗物质寻找
AMS物理目标：寻找反物质
AMS物理目标：带电宇宙线的精确测量

1409.6248

Quantitative study of the AMS-02 electron/positron spectra: implications for the pulsar and dark matter properties

Su-Jie Lin, Qiang Yuan, and Xiao-Jun Bi
Key Laboratory of Particle Astrophysics, Institute of High Energy Physics,

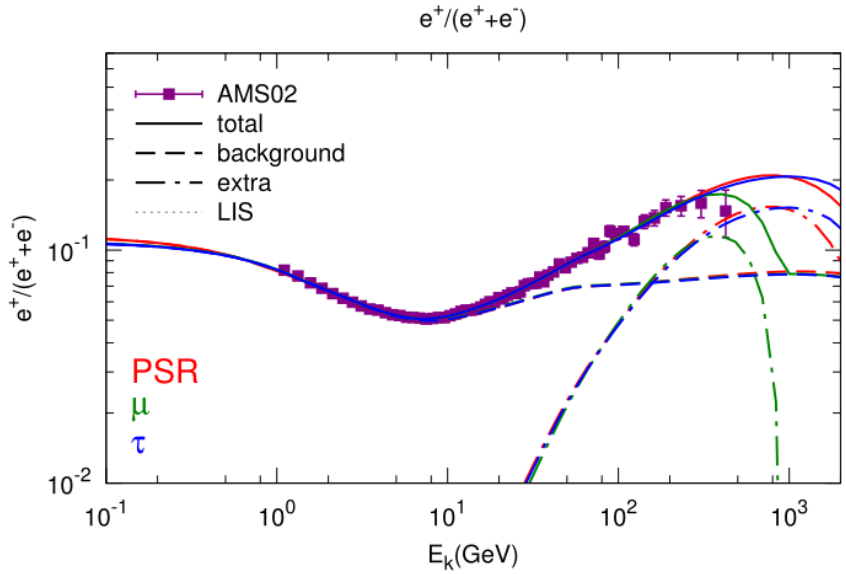

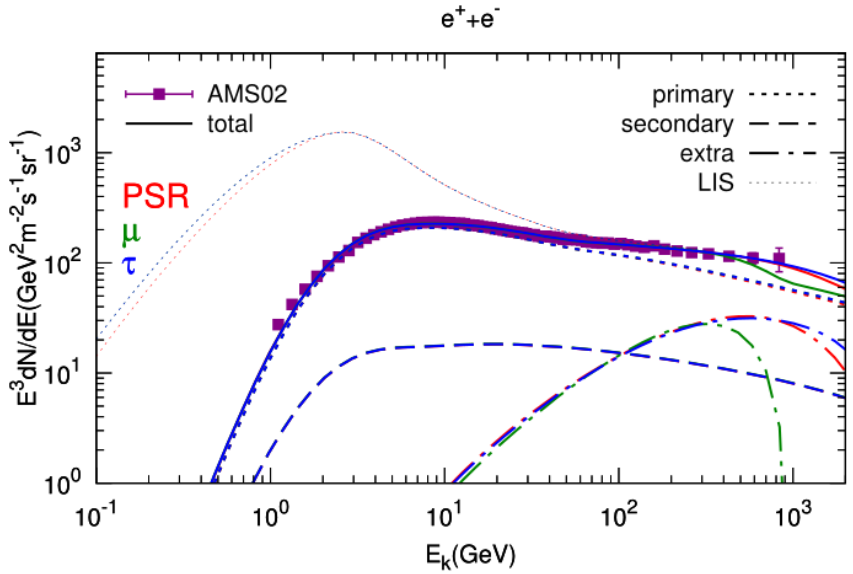

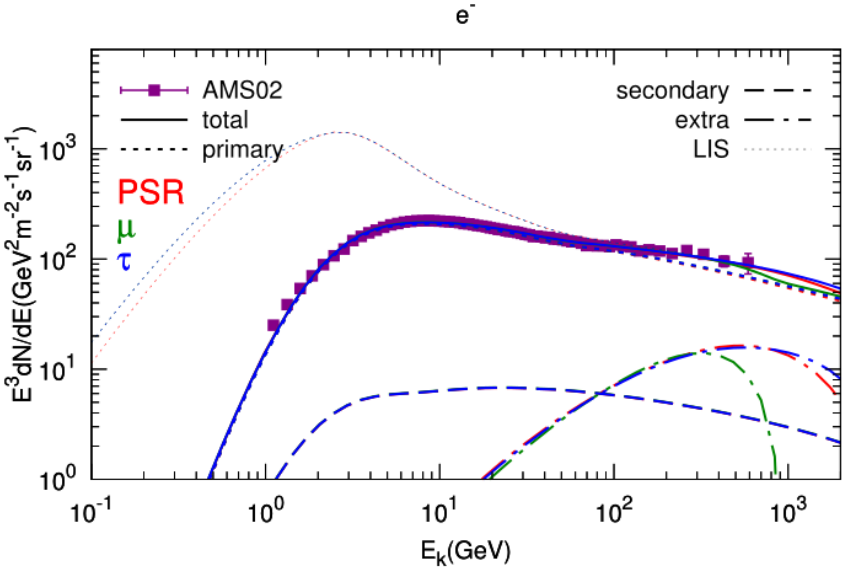

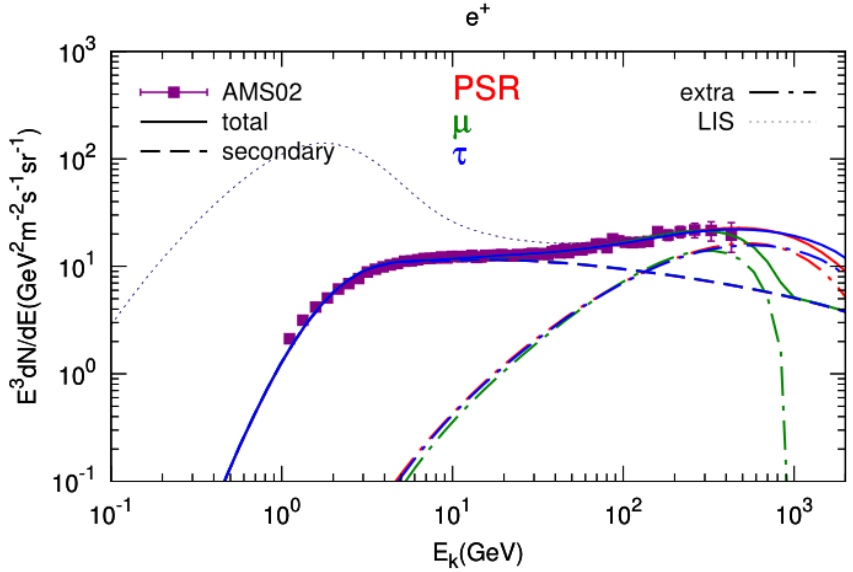

Conclusions of the quantitative study II

Both astrophysical sources, like pulsars, or dark matter can give good fit the AMS-02 data. AMS02 data can not distinguish the two scenarios.

		$\frac{\chi^2}{\text{d.o.f.}}$	χ^2	$\frac{e^+}{e^+ + e^-}$	e^-	e^+
DR	PSR	0.92	175.4	42.95	54.22	78.26
	μ	0.89	171.6	39.94	55.36	76.26
	τ	0.91	175.2	42.72	55.21	77.24
DC	PSR	0.47	88.99	51.87	14.77	22.35
	μ	1.16	223.1	88.7	46.95	87.45
	τ	0.62	118.0	59.5	21.52	37.02

Simplest view of propagation

$$G \propto \exp\left(-\frac{|\vec{x}_S - \vec{x}_\odot|^2}{\lambda_D^2}\right)$$

with $\lambda_D = \sqrt{4K_0\Delta\tilde{t}} = f(E_S, E_D)$

→ **Detection volume scaling a sphere of radius λ_D**

Figures:

galactic plane at z=0 kpc

x and y from -20 to 20 kpc

Earth located at $(x = 8, y = 0)$ kpc

2D plots of

$G(\vec{x}, 200\mathrm{GeV} \rightarrow \tilde{\mathrm{x}}_\odot, \mathrm{E}) \times \rho^2$

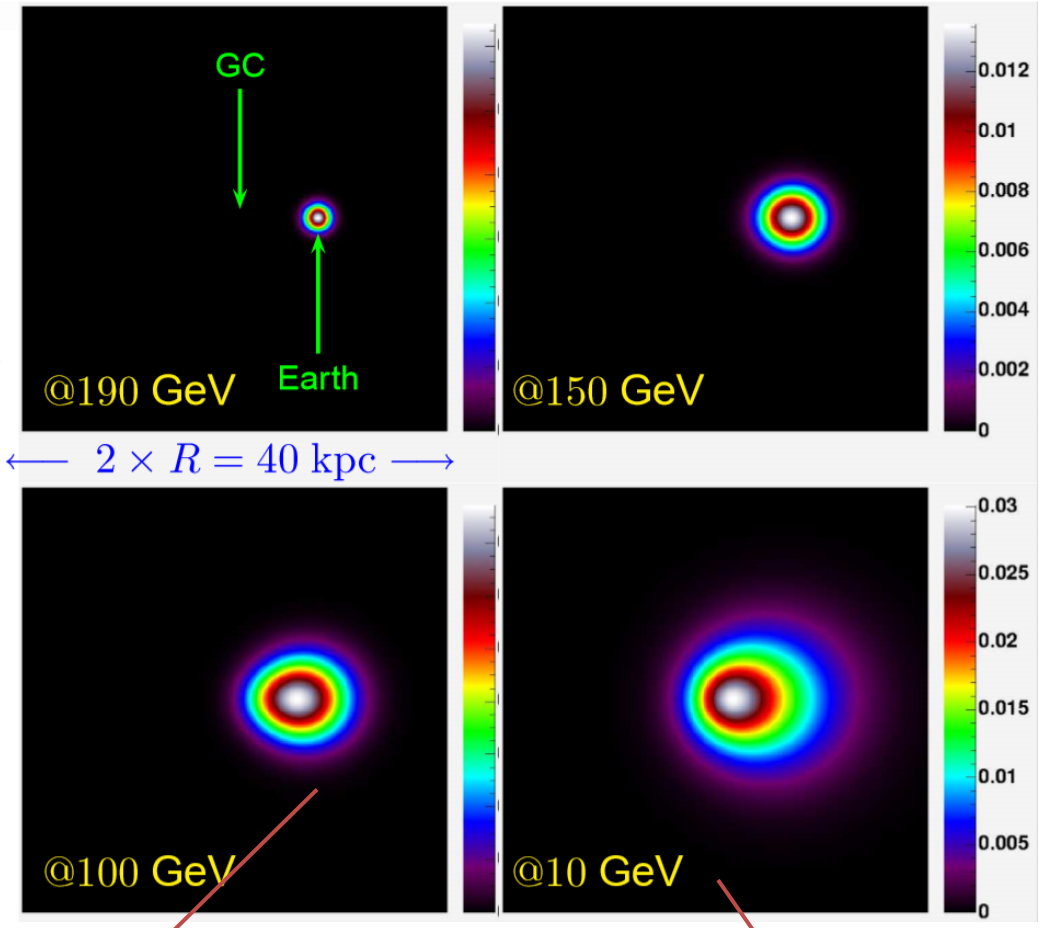

高能只能来自邻近，
具有方向性

不同源的性质不同，可能
高能电子贡献能谱的结构

Parameters of SNRs

Source	Other Name	$B_r^{1\mathrm{GHz}}$[Jy]	α_r	Size[arcmin]	r[kpc]	t[kyr]
G065.3+05.7	-	52	0.58	310×240	0.9	26
G074.0–08.5	Cygnus Loop	175	0.4	230×160	0.54	10
G114.3+00.3	-	6.4	0.49	90×55	0.7	7.7
G127.1+00.5	R5	12	0.43	45	1	[20, 30]
G156.2+05.7	-	5	0.53	110	1.0	[15, 26]
G160.9+02.6	HB9	88	0.59	140×120	0.8	[4, 7]
G203.0+12.0	Monogem Ring	-	-	-	0.3	86
G263.9–03.3	Vela YZ	varies	varies	255	0.29	11.3
G266.2–01.2	Vela Jr.	50	0.3	120	0.75	[1.7, 4.3
G328.3+17.6	Loop I (NPS)	-	-	-	0.1	200
G347.3–00.5	RXJ1713.7-3946	4	0.3	65×55	1	1.6

Flux at 3TeV

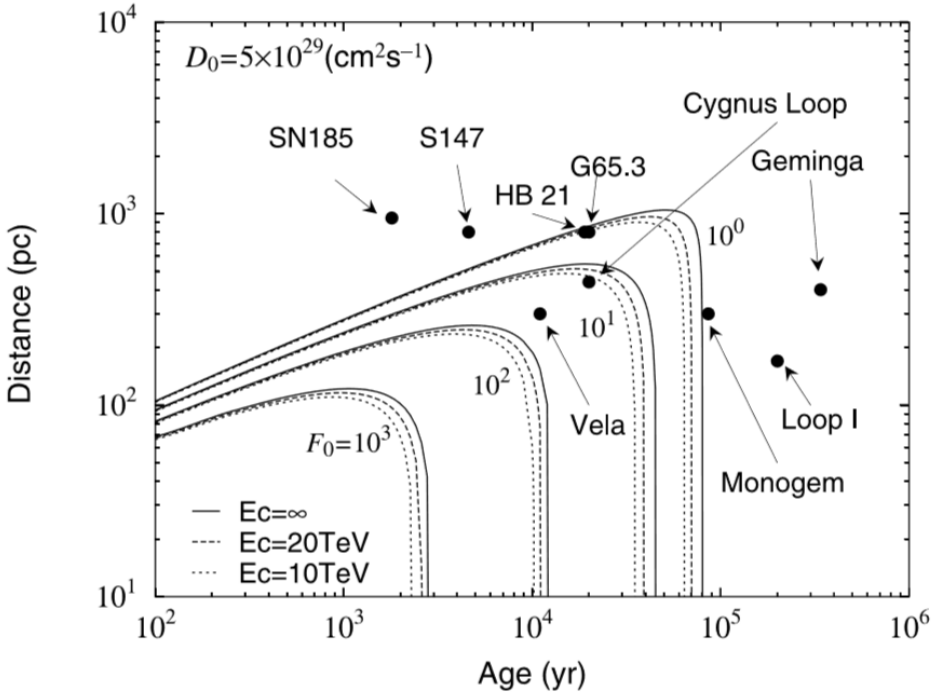

FITTING TO AMS-02

Vela YZ model

$$\alpha_{vela} = 0.519$$

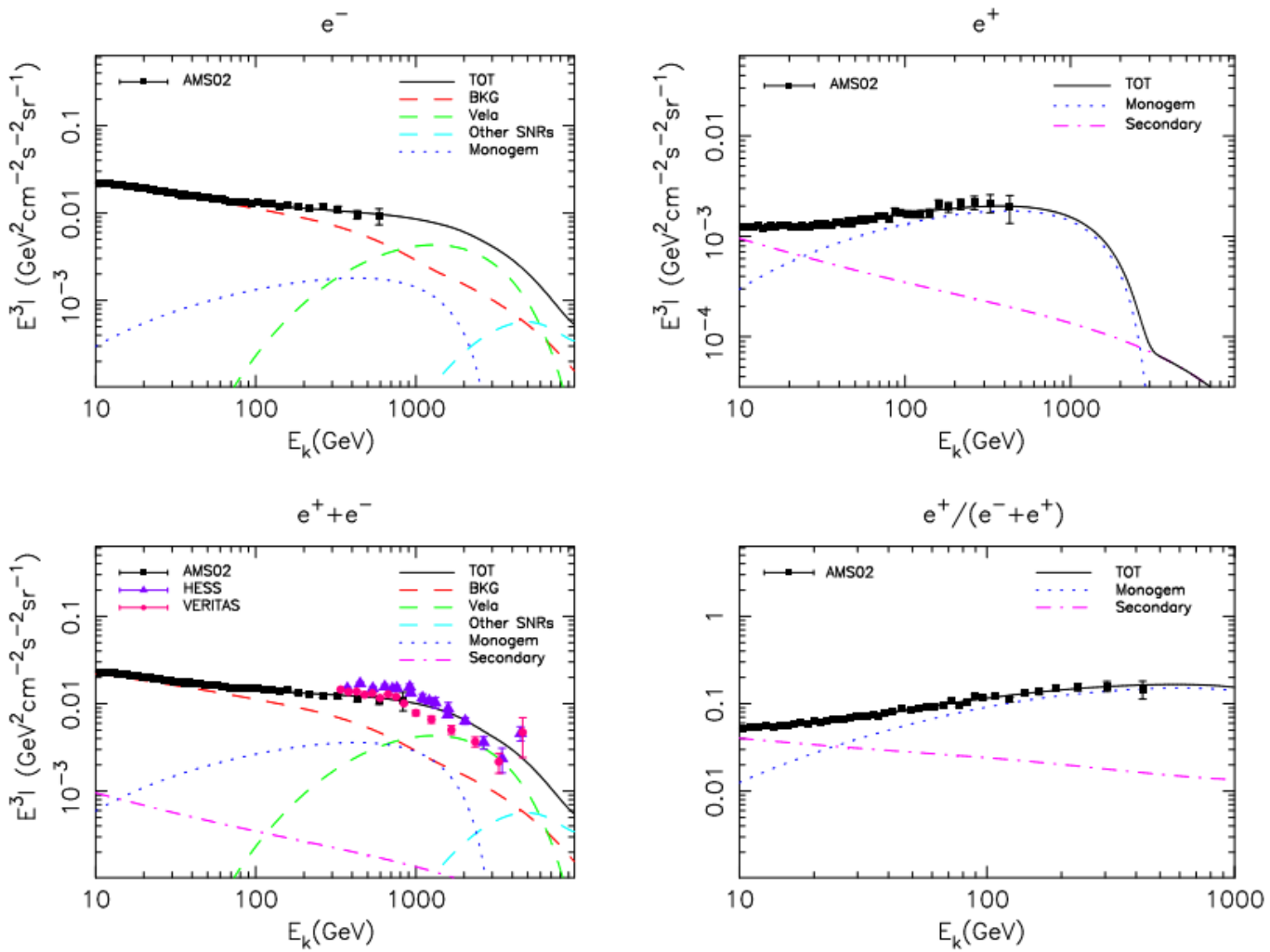

FITTING TO AMS-02

Vela YZ + Monogem Ring model (α=0.53)

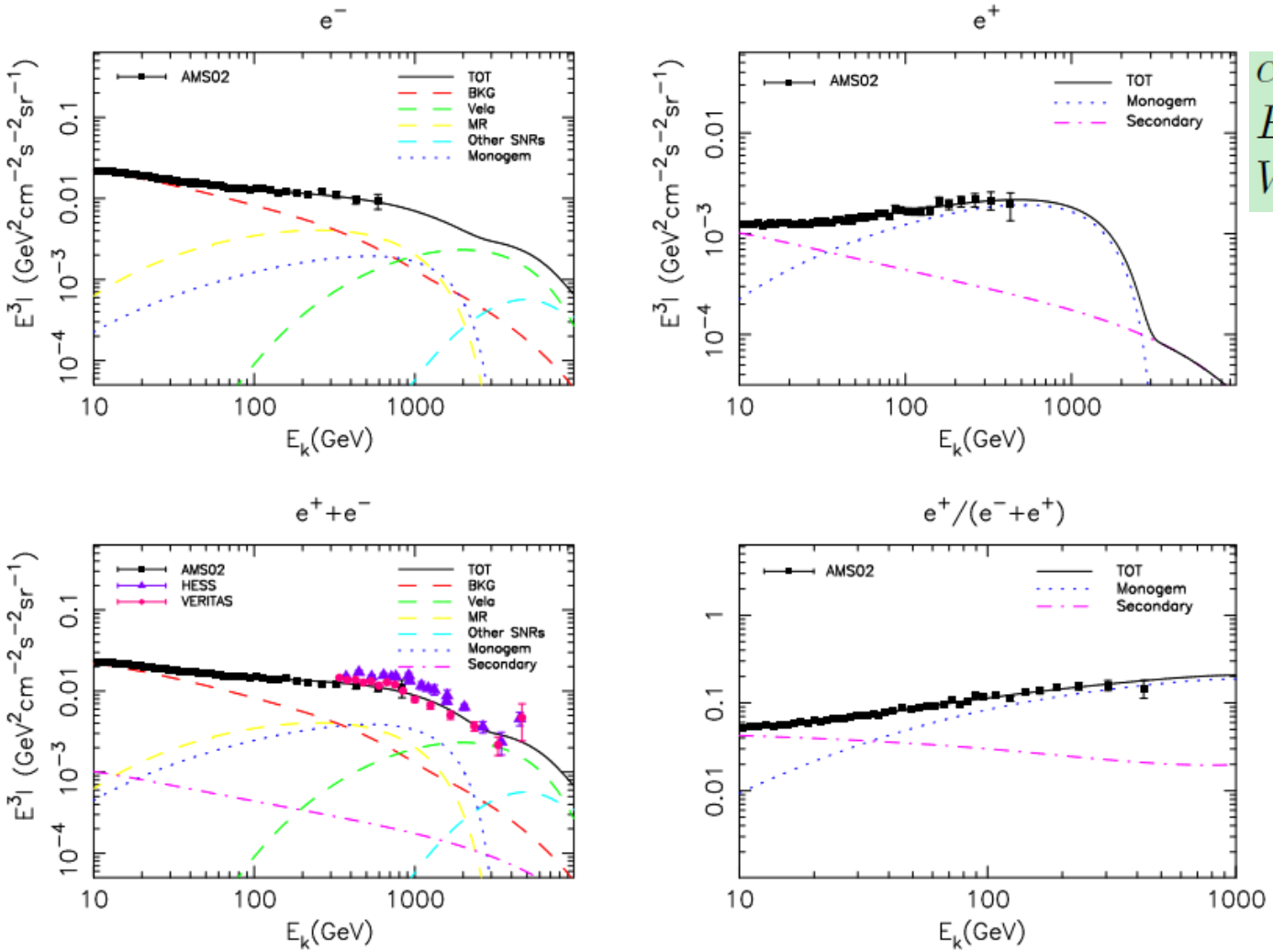

$\alpha_{mr} = 0.551$

$E_{c,mr} = 1.04$ TeV

$W_{mr} = 2.89 \times 10^{48}$ erg

FITTING TO AMS-02

Vela YZ + *Loop I* model (α=0.735)

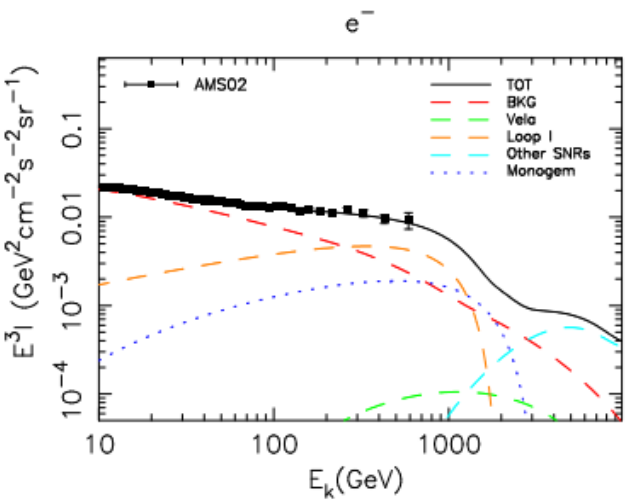

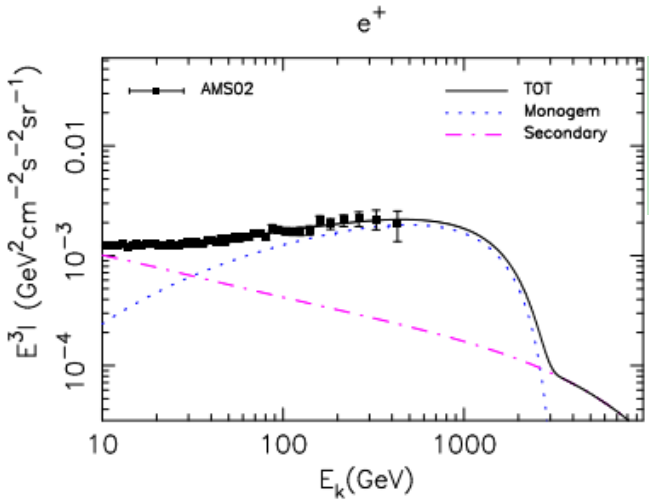

$\alpha_{loop} = 0.417$
$E_{c,loop} = 1.49$ TeV
$W_{loop} = 5.08 \times 10^{48}$ erg

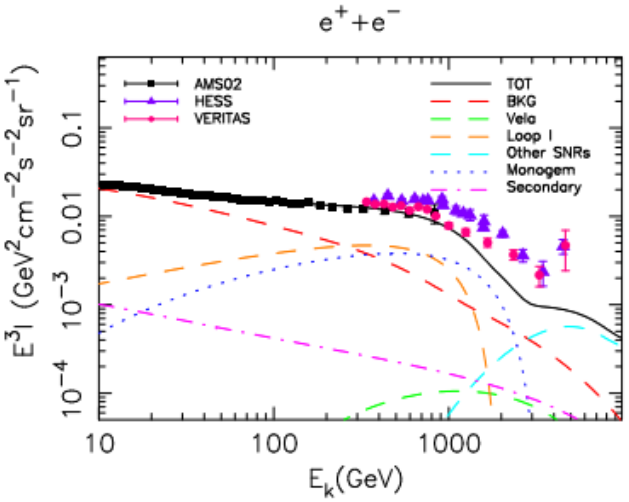

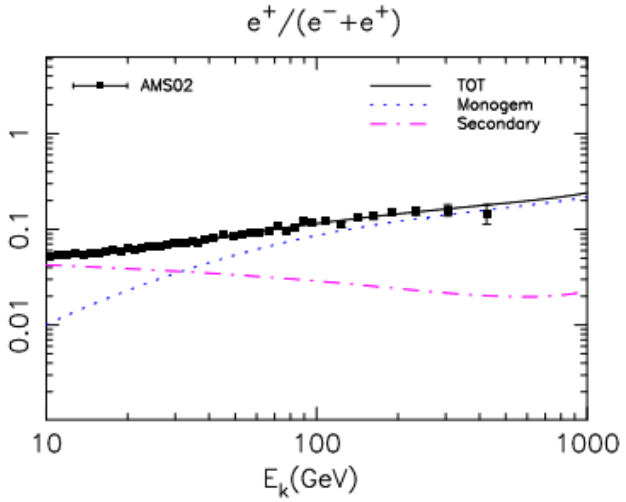

Strong constraints on the vela XY contribution to AMS-02 lepton data

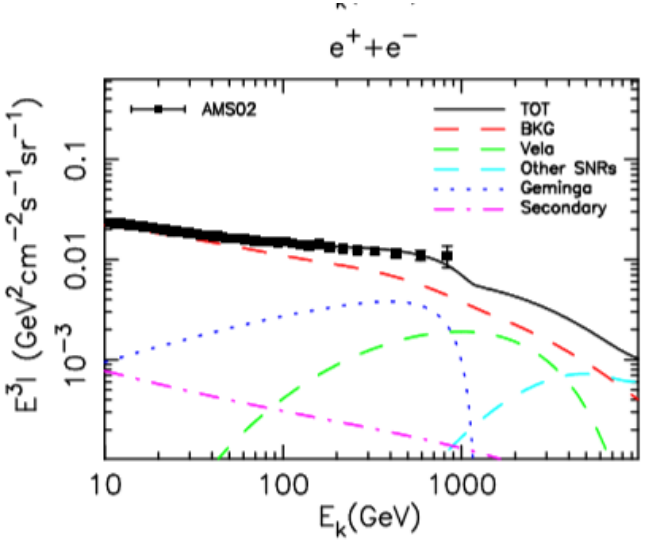

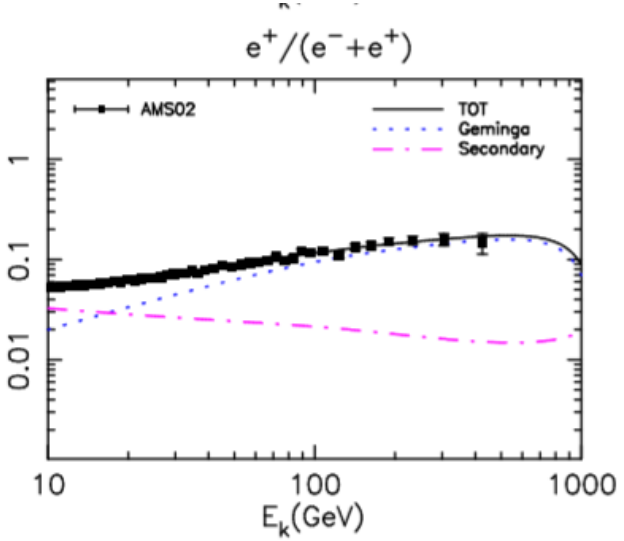

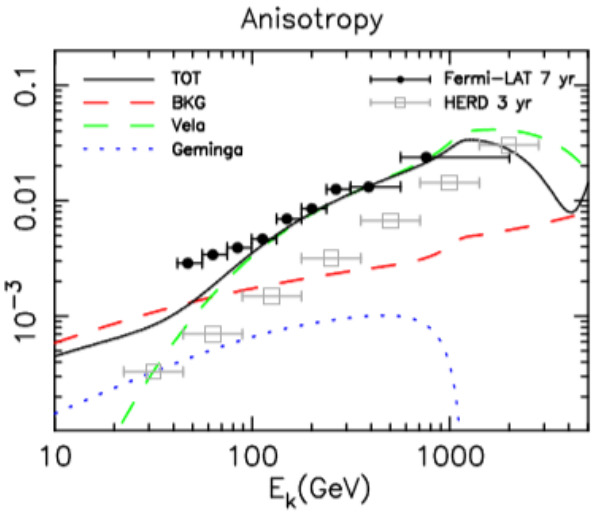

Fitting to present data implies constraint from HERD

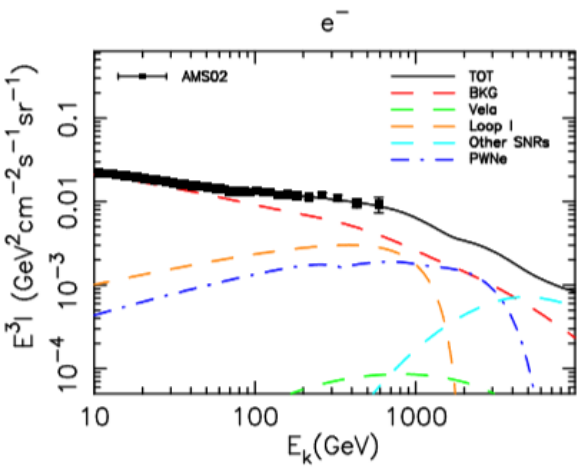

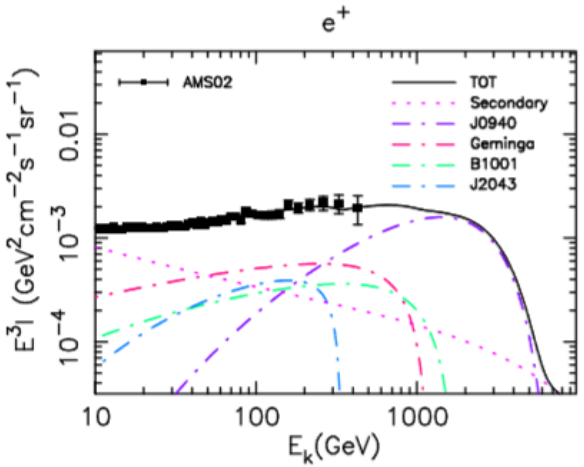

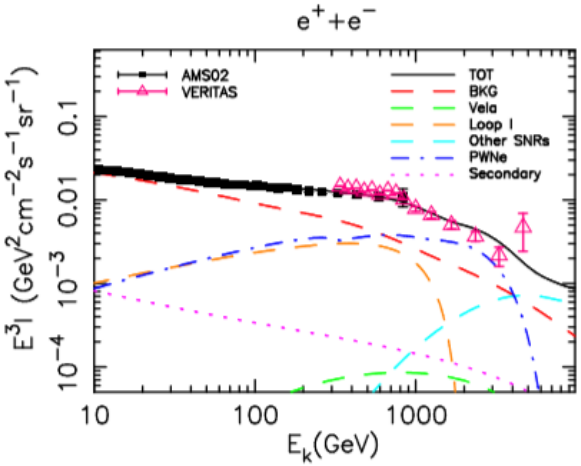

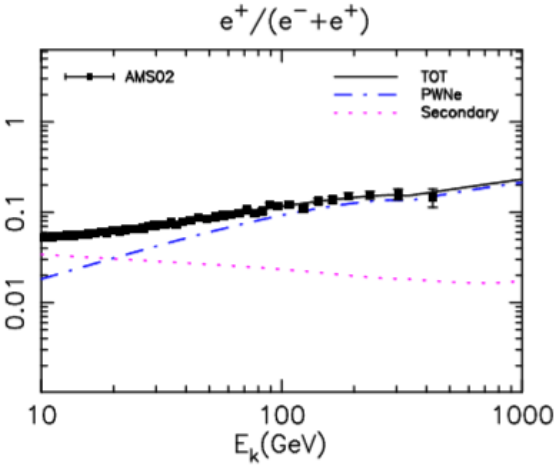

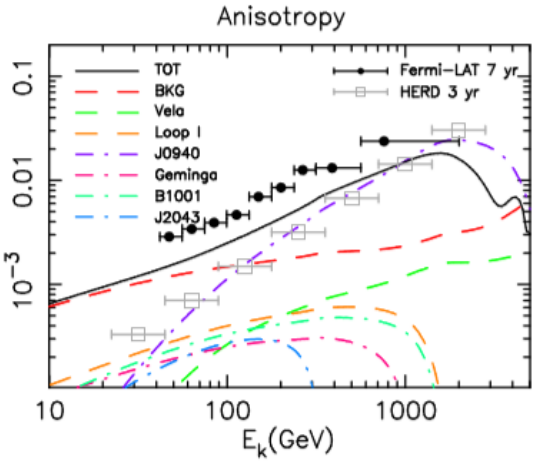

Predictions above TeV

Vela YZ

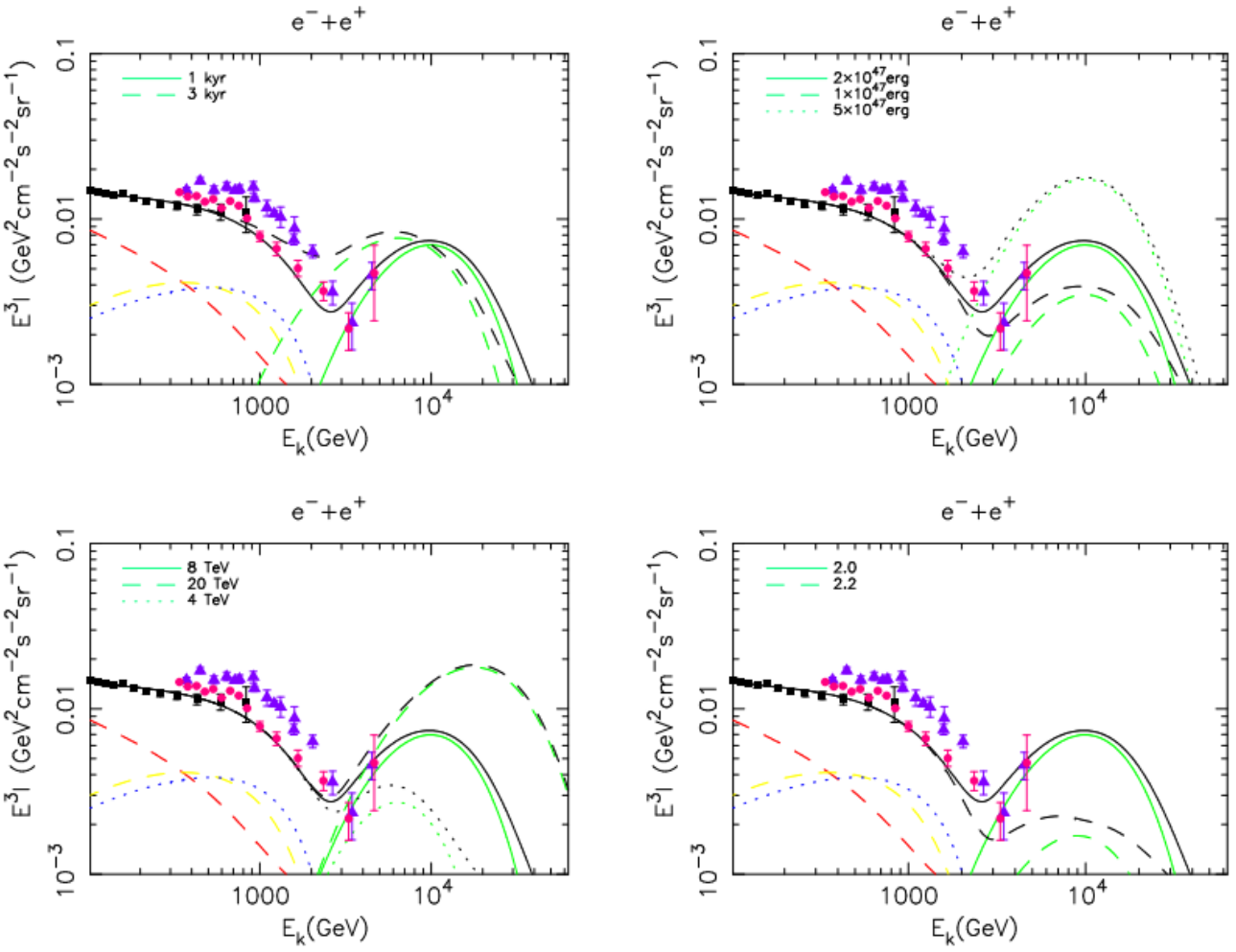

top left:

$t = 1,\ 3$ kyr

top right:

$W = (1,\ 2,\ 5) \times 10^{47}$ erg

bottom left:

$E_c = 4,\ 8,\ 20$ TeV

bottom right:

$\gamma = 2.0,\ 2.2$

Predictions above TeV from Vela X

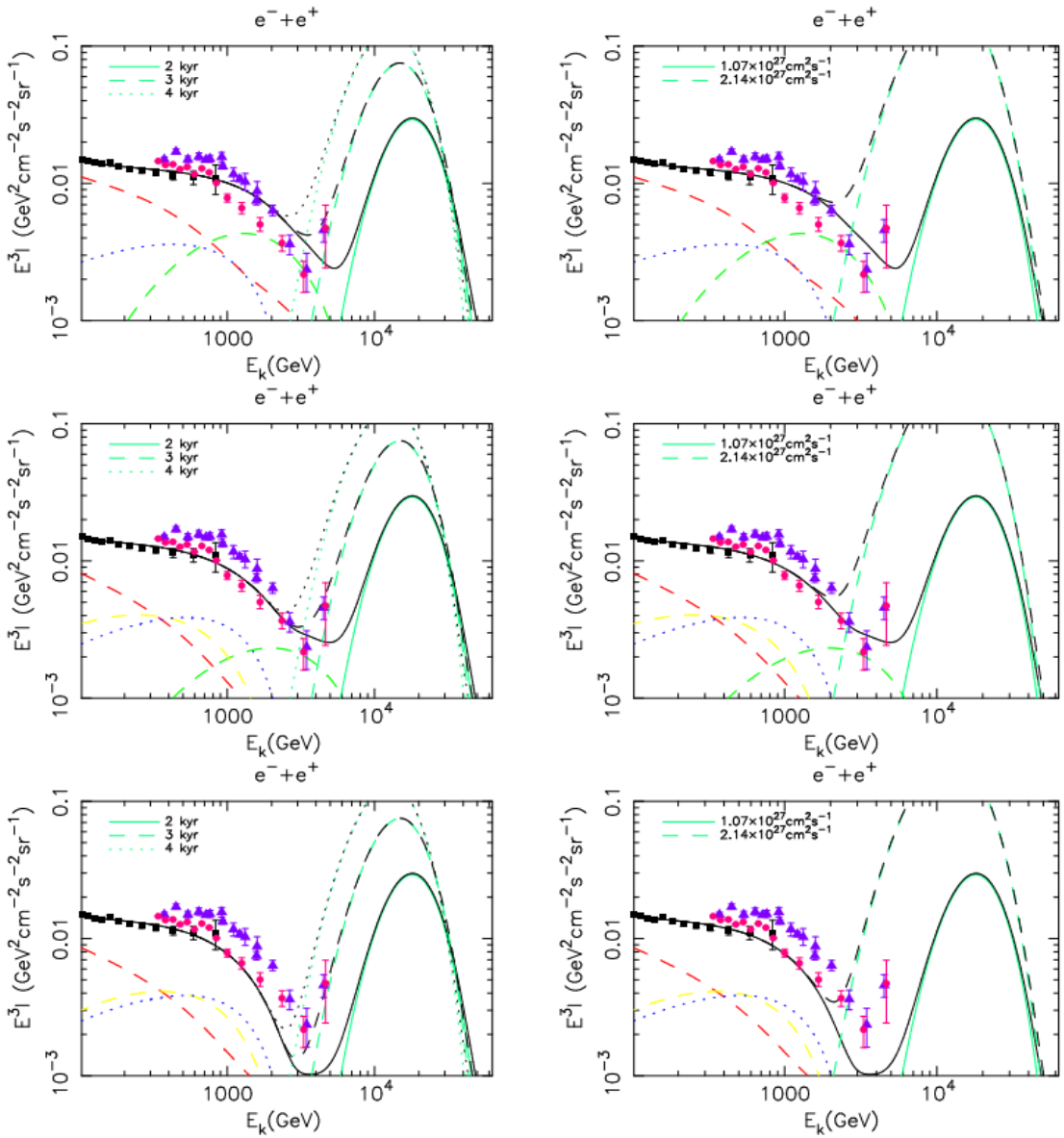

left:

$t = 2,\ 3,\ 4$ kyr

right:

$D_0 = (1.07, 2.14) \times 10^{27}\ \mathrm{cm}^2\ \mathrm{s}^{-1}$

High energy bump and anisotropy constraint by Fermi and HERD

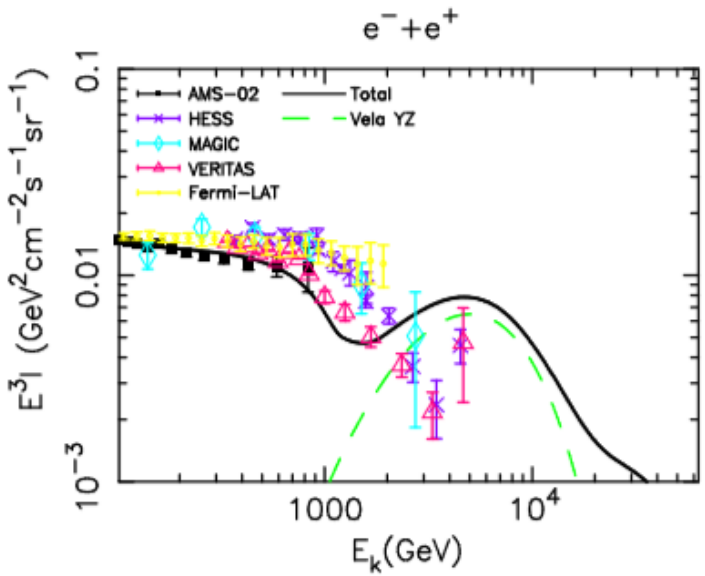

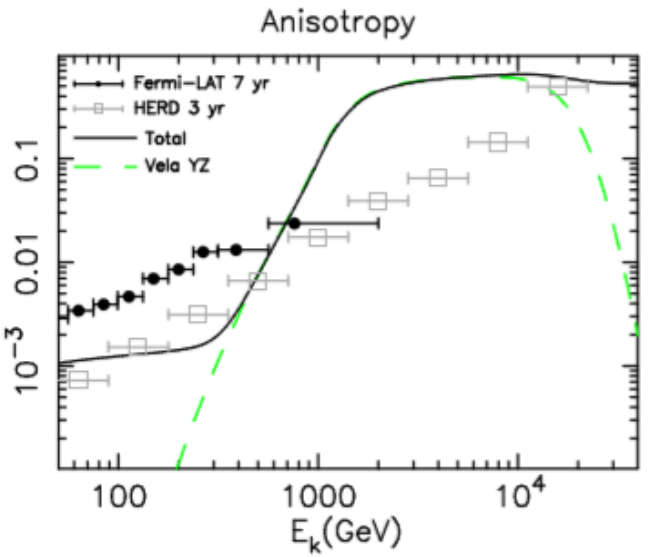

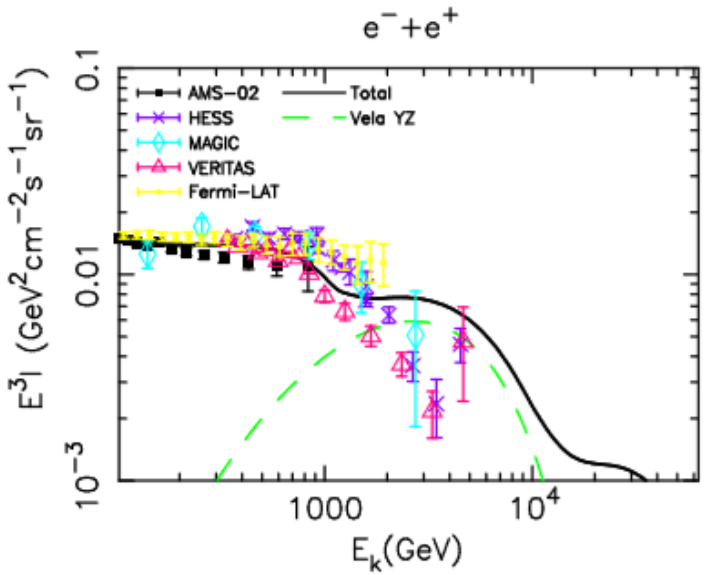

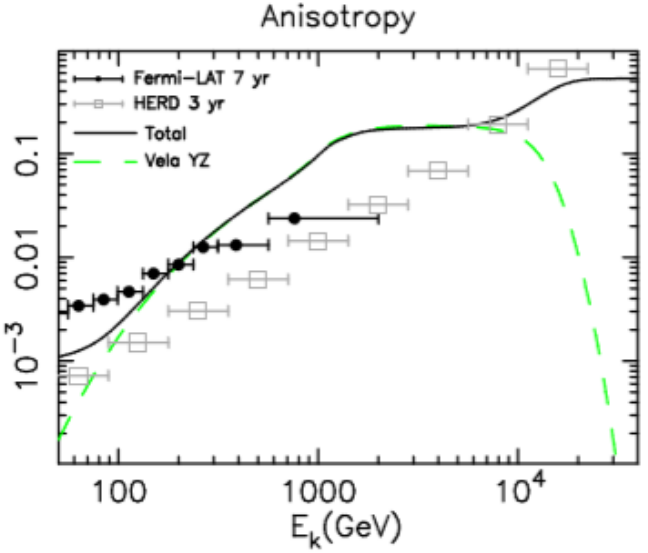

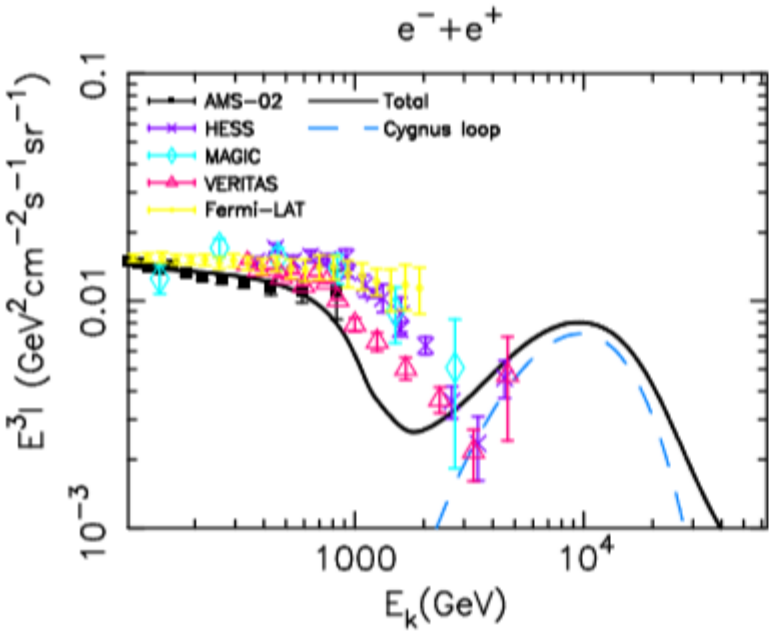
e^-+e^+
AMS−02
HESS
MAGIC
VERITAS
Fermi−LAT
Total
Cygnus loop
E^3I (GeV^{2}cm^{-2}s^{-1}sr^{-1})
0.1
0.01
10^{-3}
1000
10^4
E_k(GeV)

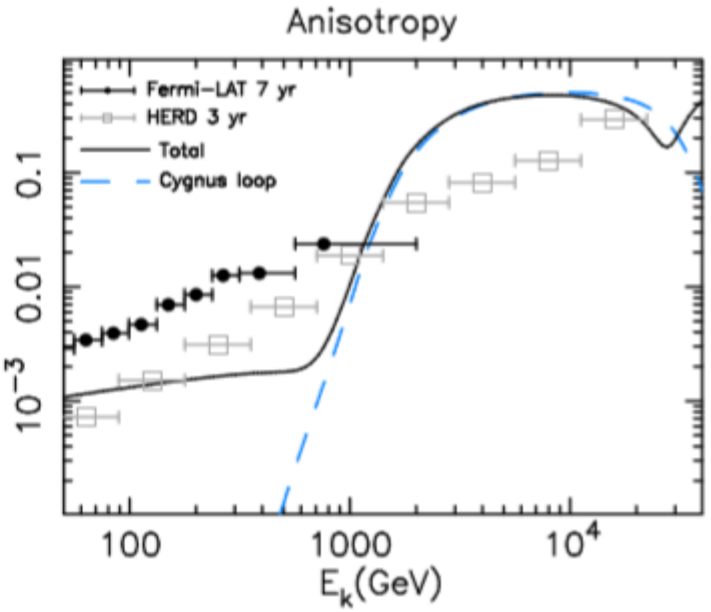
Anisotropy
Fermi−LAT 7 yr
HERD 3 yr
Total
Cygnus loop
0.1
0.01
10^{-3}
100
1000
10^4
E_k(GeV)

AMS $\bar{p}/p$ results

AMS-02 pbar/p

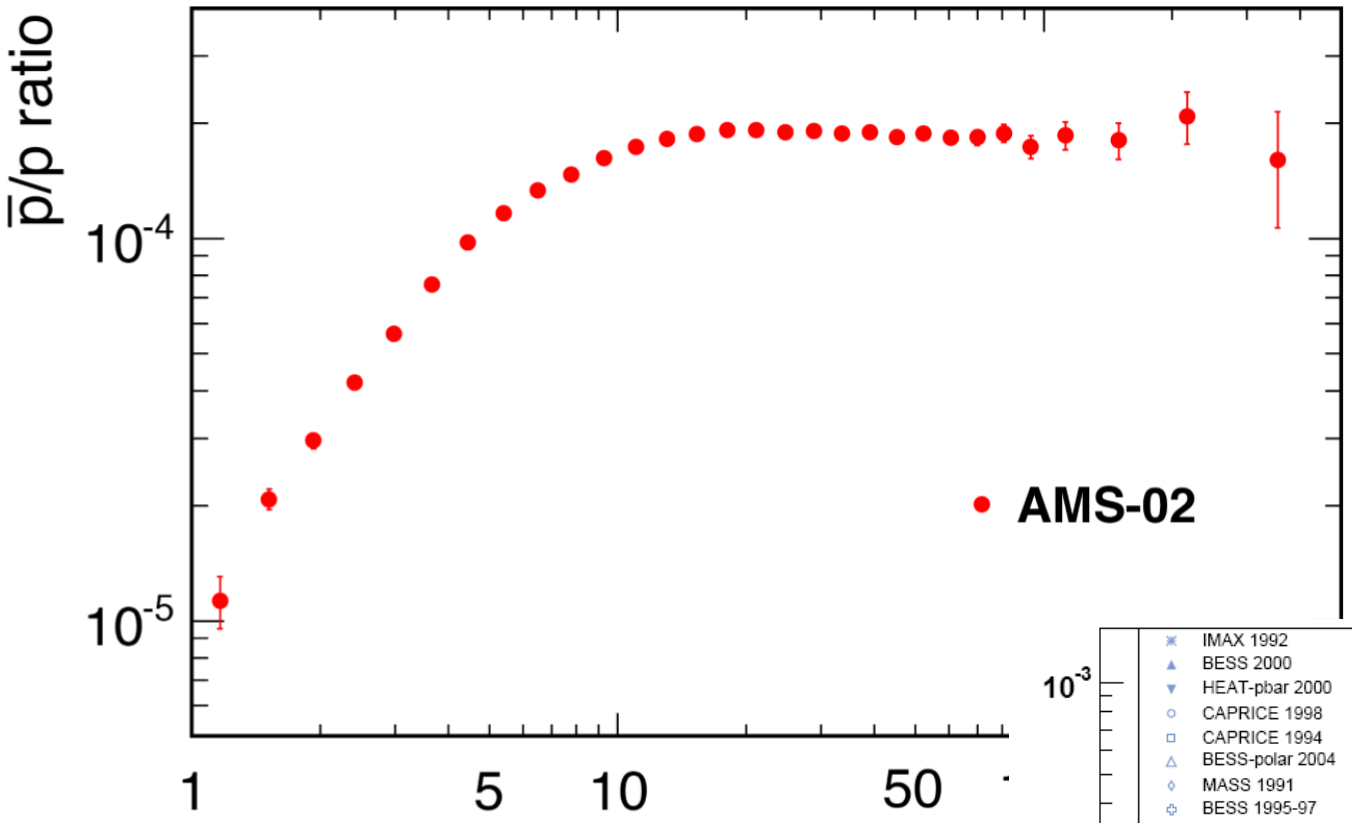

PAMELA pbar/p

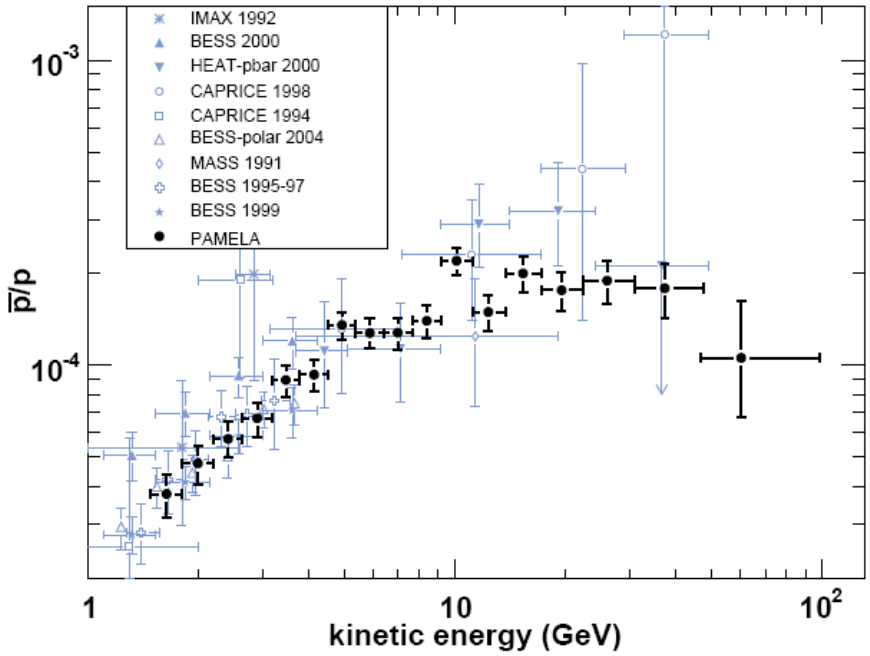

Anti-proton ratio

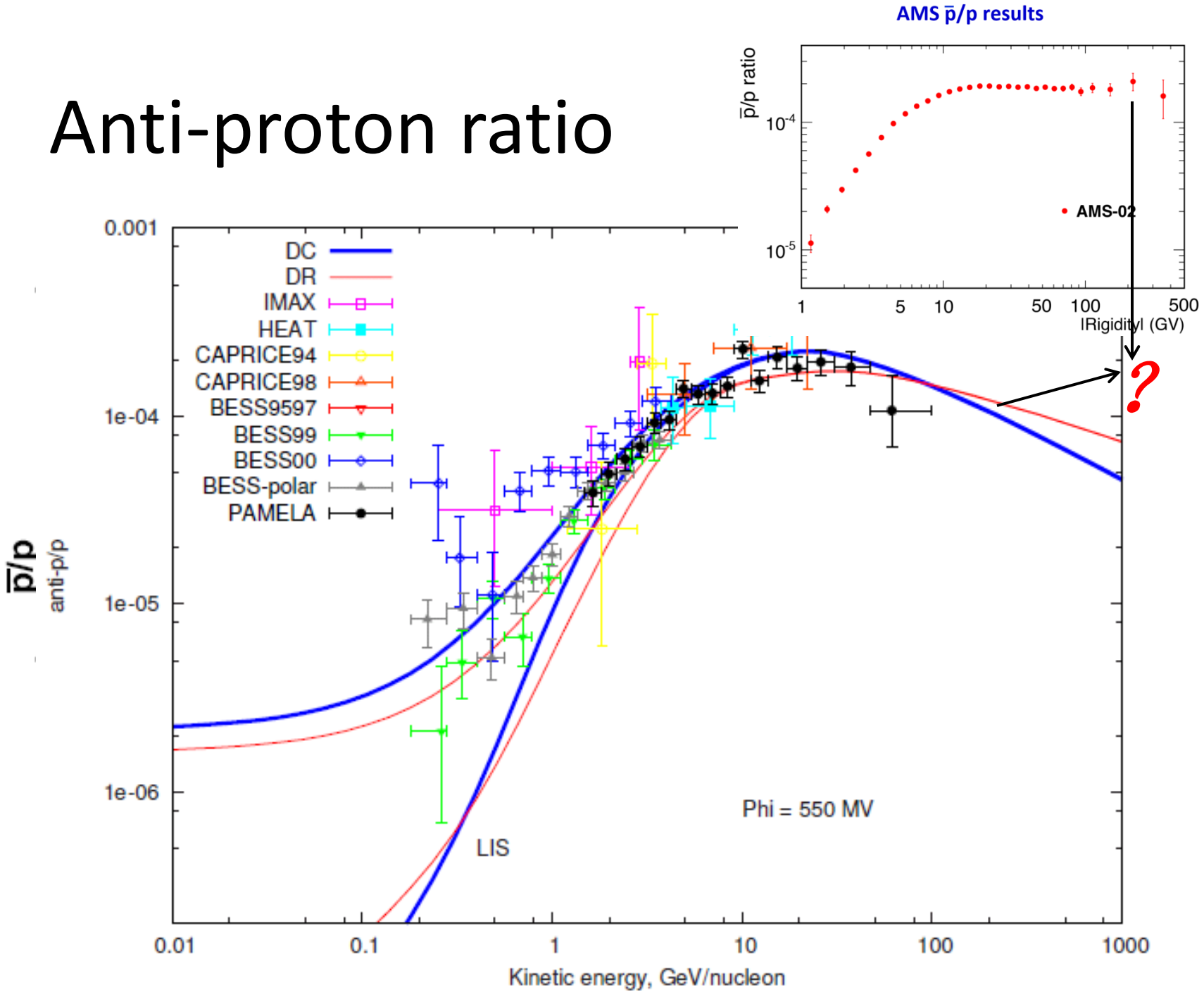

AMS-02 pbar/p

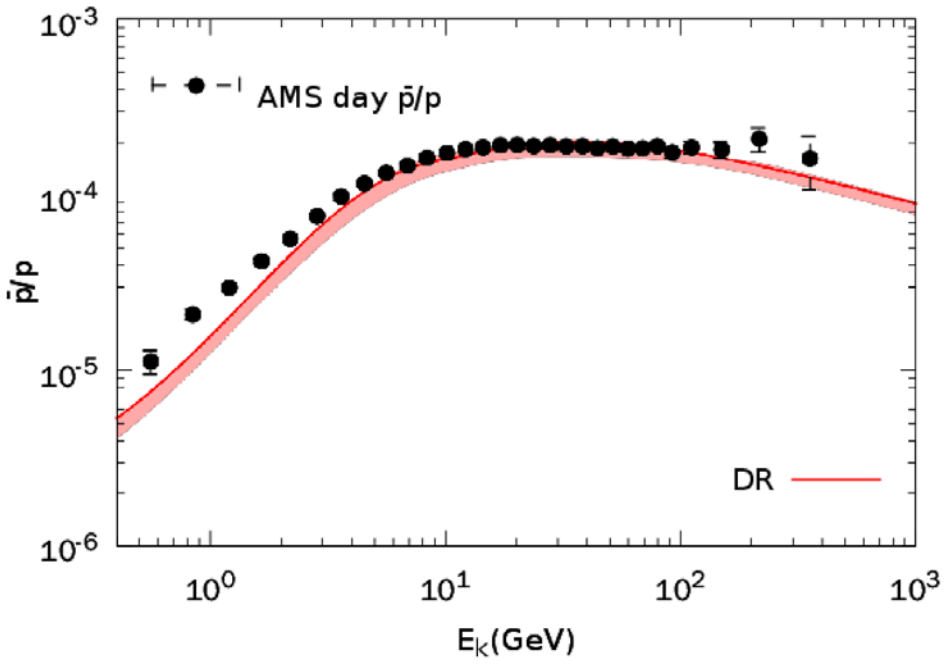

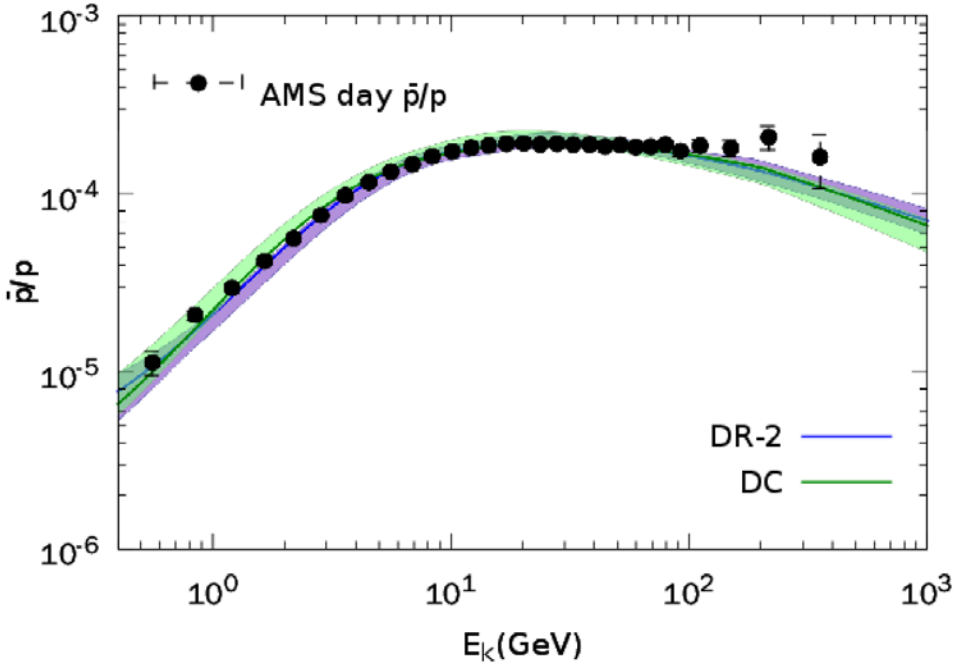

Calculation seems predict some excess at high energies. However, the prediction is based on an old hadronic interaction model.

相互作用模型的不确定性

NA49(2010) p(158GeV/c) + p - > ap

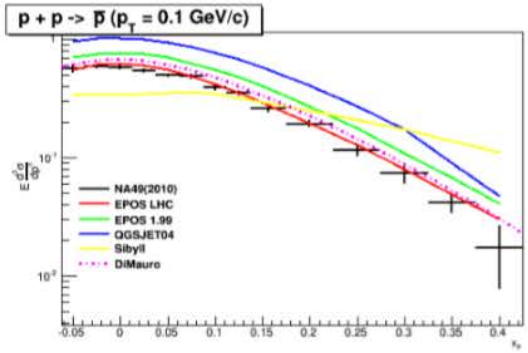

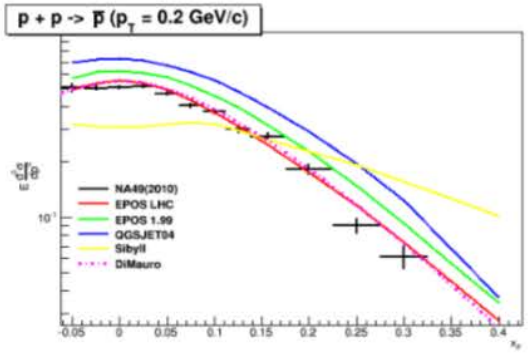

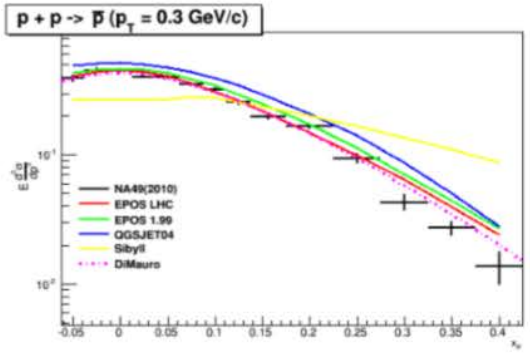

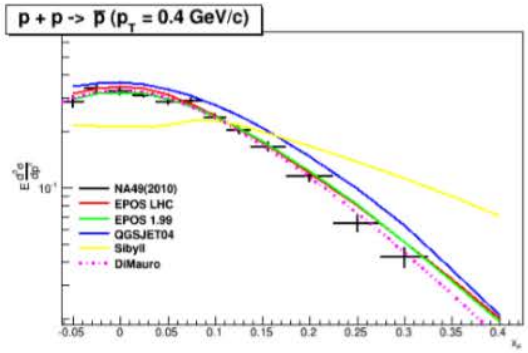

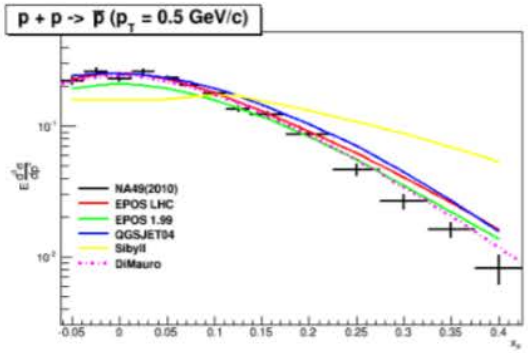

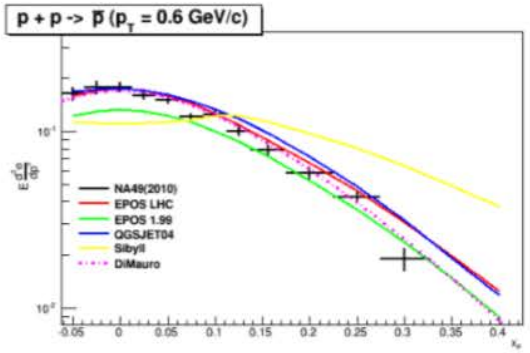

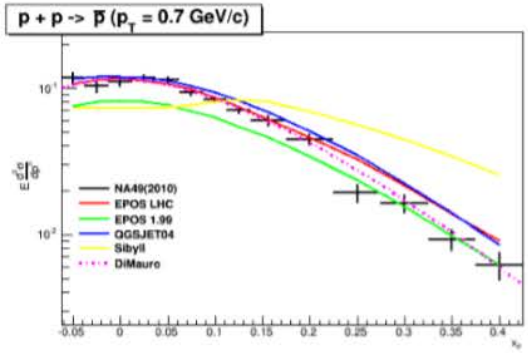

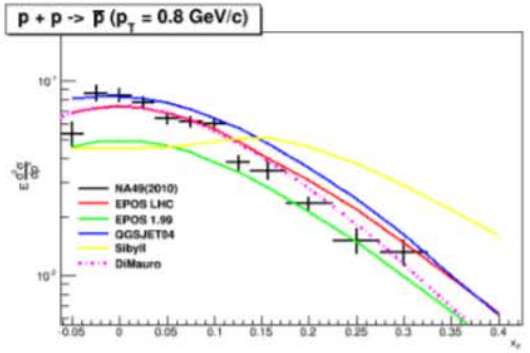

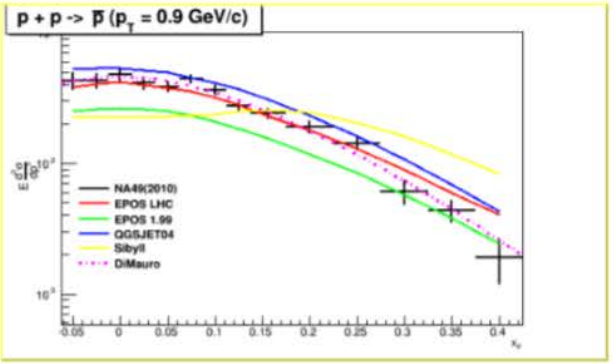

相互作用模型不确定性

NA49(2012) p(158GeV/c) + C - > ap

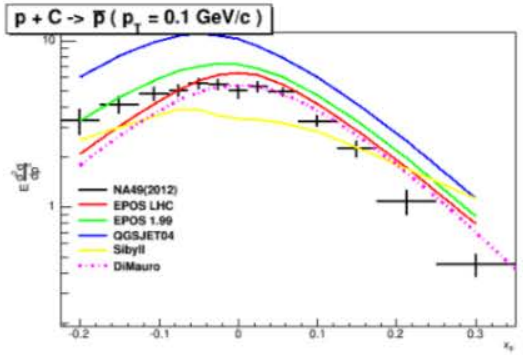

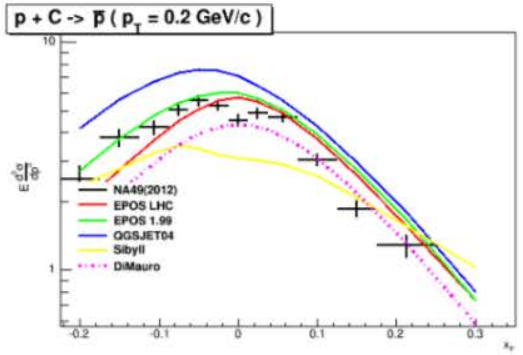

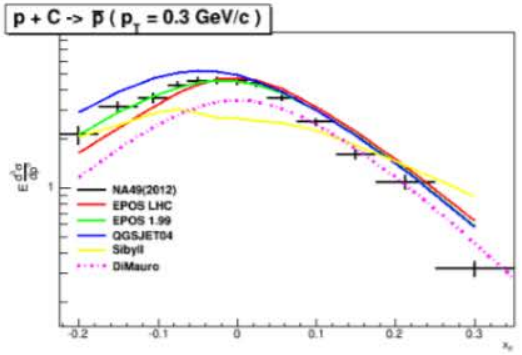

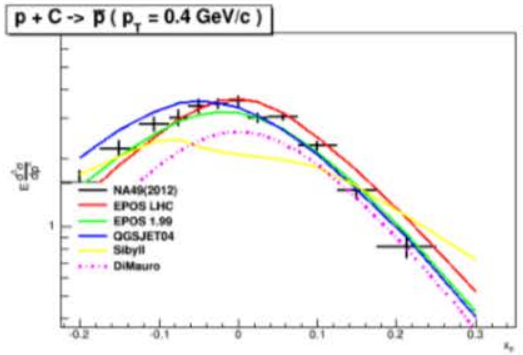

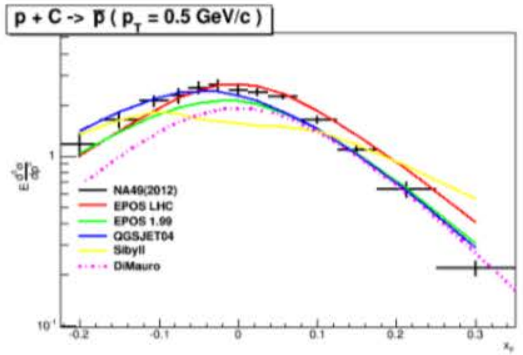

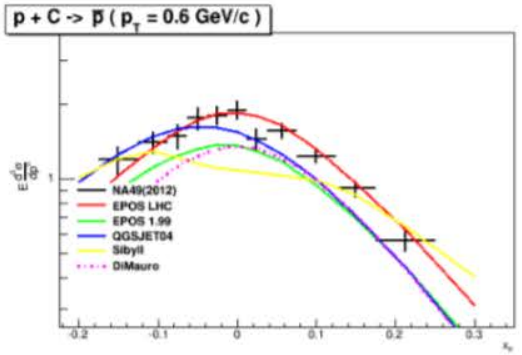

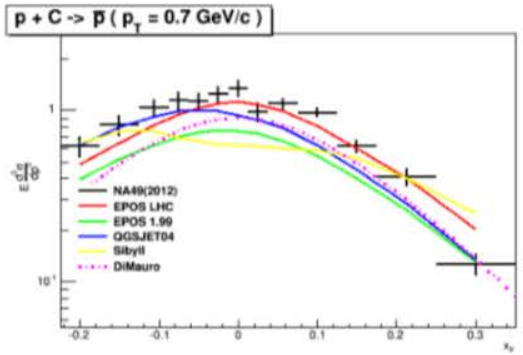

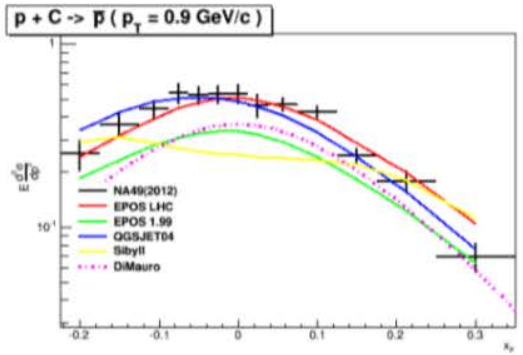

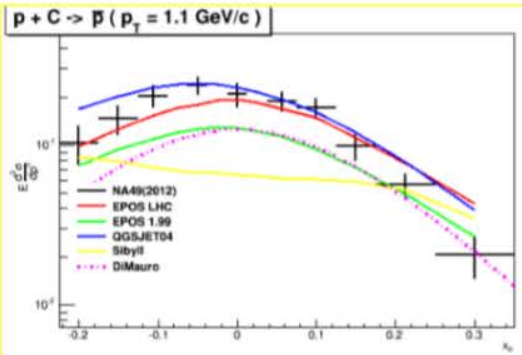

Pbar/p adopting different interaction model

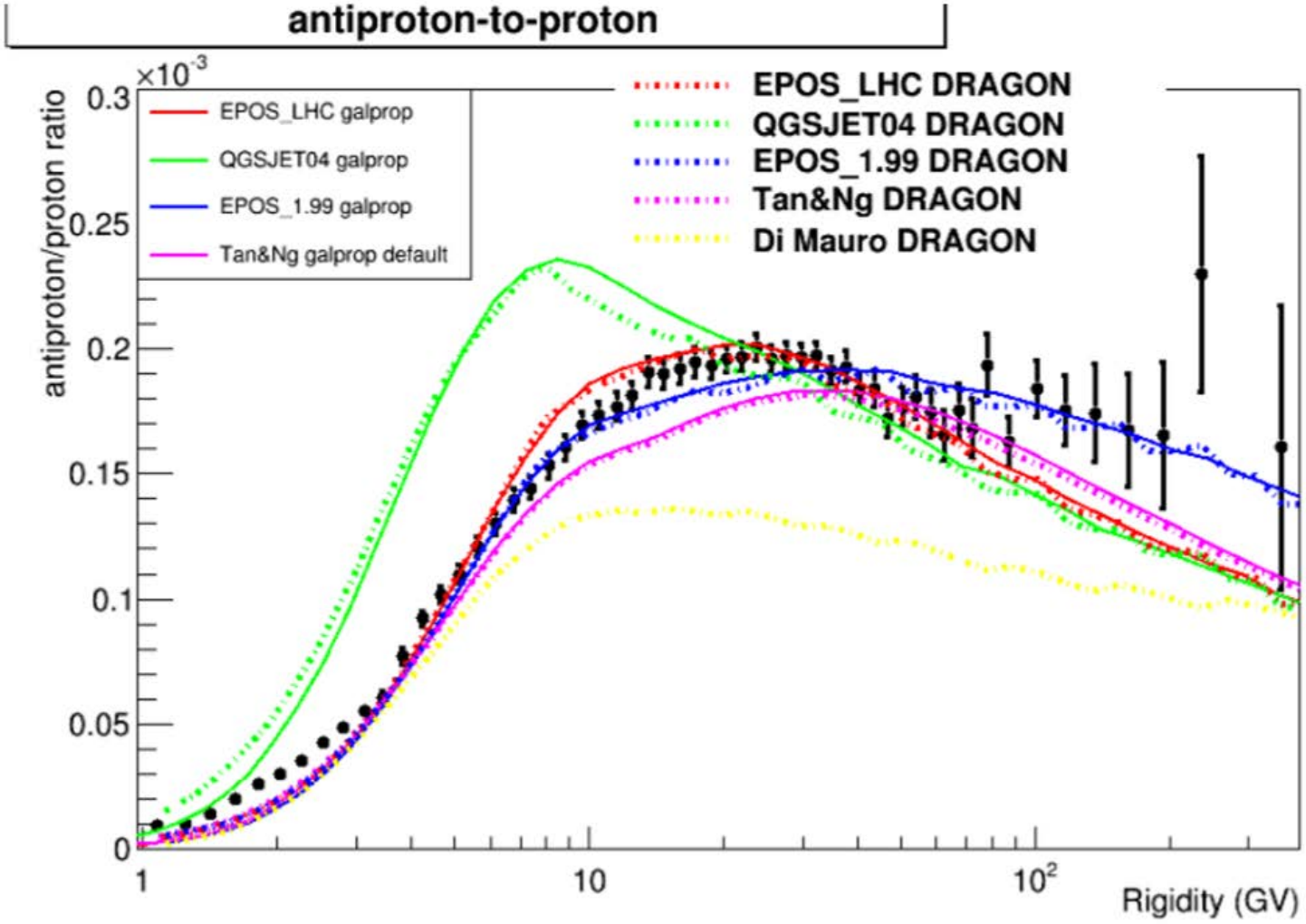

Pbar/p adopting different interaction model

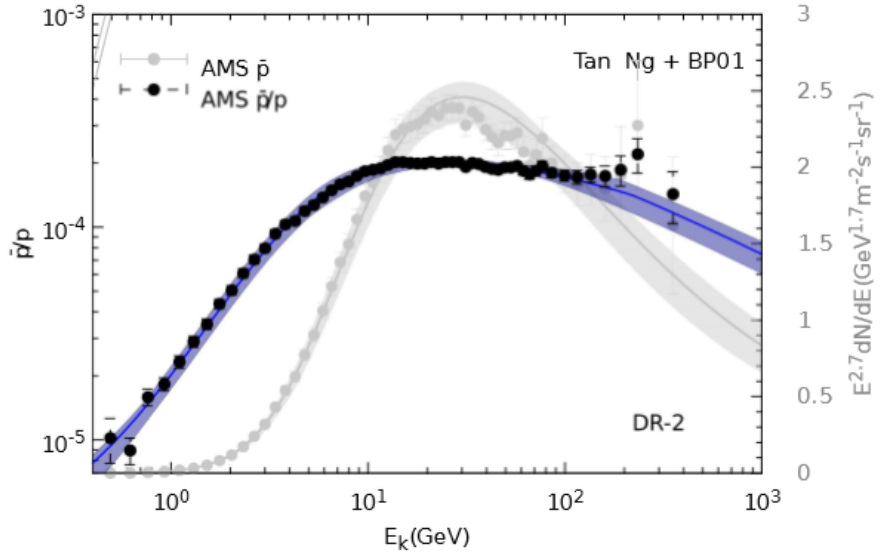

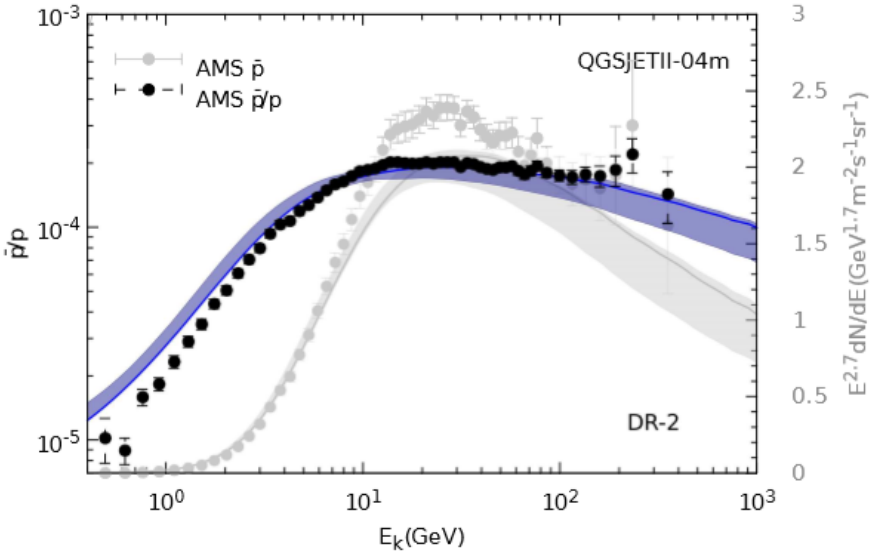

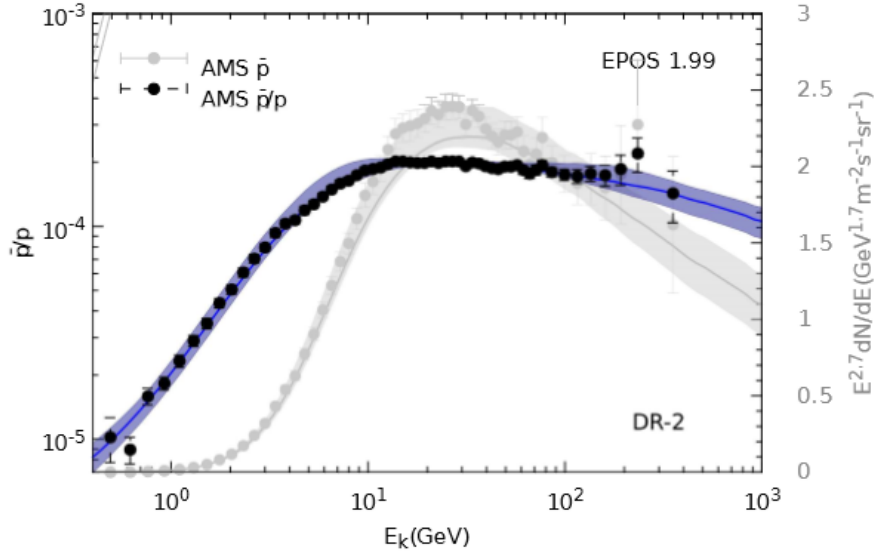

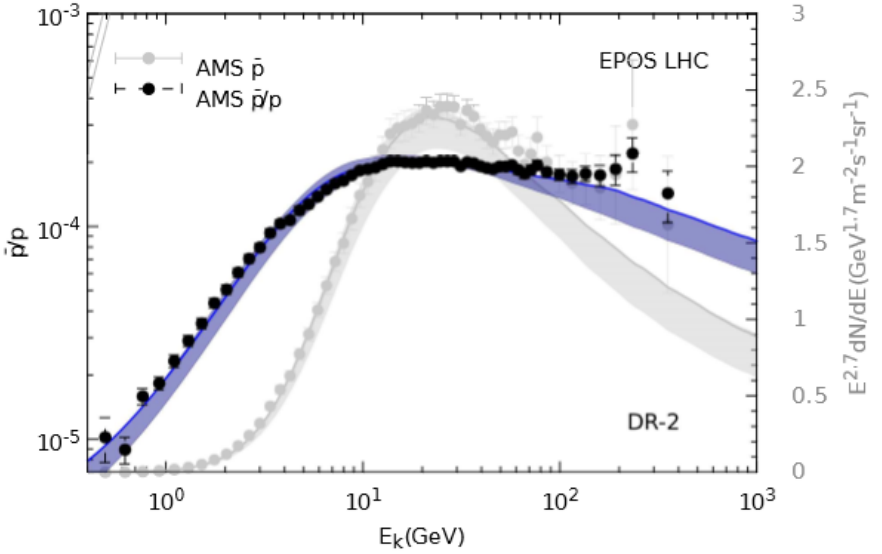

暗物质卫星简介

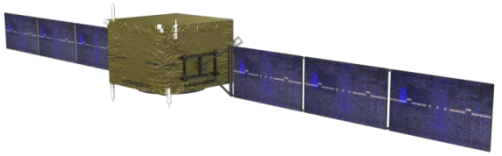

- 暗物质粒子探测卫星（简称DAMPE）是中国科学院空间科学先导专项之一，其主要科学目标是开展高能电子、宇宙线粒子和伽玛射线的观测，进而探寻暗物质存在的证据，并研究其空间分布特性，同时也可开展高能宇宙线、伽马天文的研究。

- 该卫星于2015年12月17日发射。发射后，在轨测试标定工作1~2个月，之后进入常管模式。

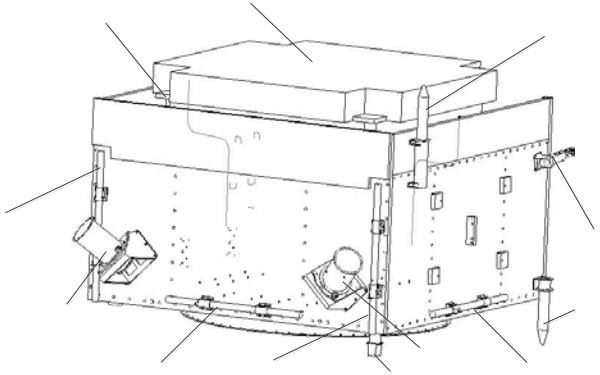

高能电子探测指标

- 探测能区：5～10,000GeV；
- 能量分辨率：1.5%@800GeV；
- 本底抑制能力：大于100,000；
- 几何因子：大于0.3m^2.sr。

HERD concept

- **Aim: a flagship and landmark scientific experiment onboard the China's Space Station**
- **Sciences**
  - Indirect dark matter search with unprecedented sensitivity
  - Precise cosmic ray spectrum and composition measurements up to the knee energy
  - Gamma-ray monitoring and survey
- **Unique capabilities**
  - Direct PeV CR observation with best energy resolution
  - Low energy gamma ray observation
  - Largest geometric factors for electrons and cosmic rays
- **Planned launch 2022-2025; 10+ years lifetime**

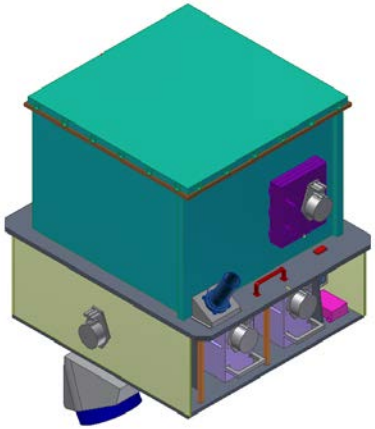

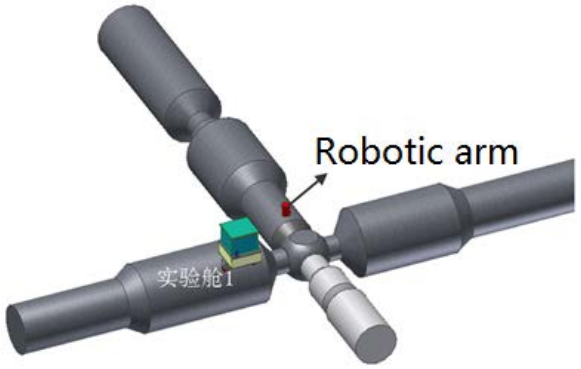

e^{+-} propagation

- For e^{+-} , the most relevant process is energy loss $$\partial_t \mathcal{N} - \boldsymbol{\nabla} \cdot \{K(E) \boldsymbol{\nabla} \mathcal{N}\} + \partial_E \left\{ \frac{dE}{dt} \mathcal{N} \right\} = \mathcal{Q}(E, \boldsymbol{x}, t)$$
- The Green function for steady states is
- $$\mathcal{G}(\boldsymbol{x}, E \leftarrow \boldsymbol{x}_s, E_s) = \frac{1}{b(E)\,(\pi\,\lambda^2)^{\frac{3}{2}}} \cdot \exp\left\{ -\frac{(\boldsymbol{x}_s - \boldsymbol{x})^2}{\lambda^2} \right\}$$

$$b(E) \equiv -\frac{dE}{dt}\ ;\ \ \lambda^2 \equiv 4 \int_E^{E_s} dE' \frac{K(E')}{b(E')}$$

- They are in power-law form

$$K(E) \equiv \beta K_0 \left(\frac{\mathcal{R}}{1\,\mathrm{GV}}\right)^{\delta} \simeq K_0\,\epsilon^{\delta}$$

$$b(E) \equiv b_0\,\epsilon^{\alpha} = \frac{E_0}{\tau_l}\,\epsilon^{\alpha} \;\text{ with }\; \epsilon \equiv \frac{E}{E_0 = 1\,\mathrm{GeV}}$$

- We get for $\mathcal{G} \propto E^{\frac{\alpha}{2} - \frac{3}{2}(\delta+1)}$;

- For secondaries it is source form

$$\mathcal{Q}(E, \boldsymbol{x}) = 2\, h^{'}\, \mathcal{Q}_0\, \delta(z)\, \epsilon^{-\gamma}$$

- The propagated flux is

$$\phi_{\odot}(E) \simeq \frac{o\, c\, h}{2\, \pi^{3/2}} \frac{\mathcal{Q}_0}{\sqrt{K_0/\tau_l}} \epsilon^{-\widetilde{\gamma}}$$

- The index is

$$\widetilde{\gamma} = \gamma + \frac{1}{2}(\alpha + \delta - 1)$$

- For the observed $\widetilde{\gamma} \approx 3$ we have γ=[2.1,2.35] for $\delta \in [0.3, 0.8]$.

Secondary electron/positron

- The calculated flux of secondary electrons and positrons are
- Numerical calculation of spectrum is needed

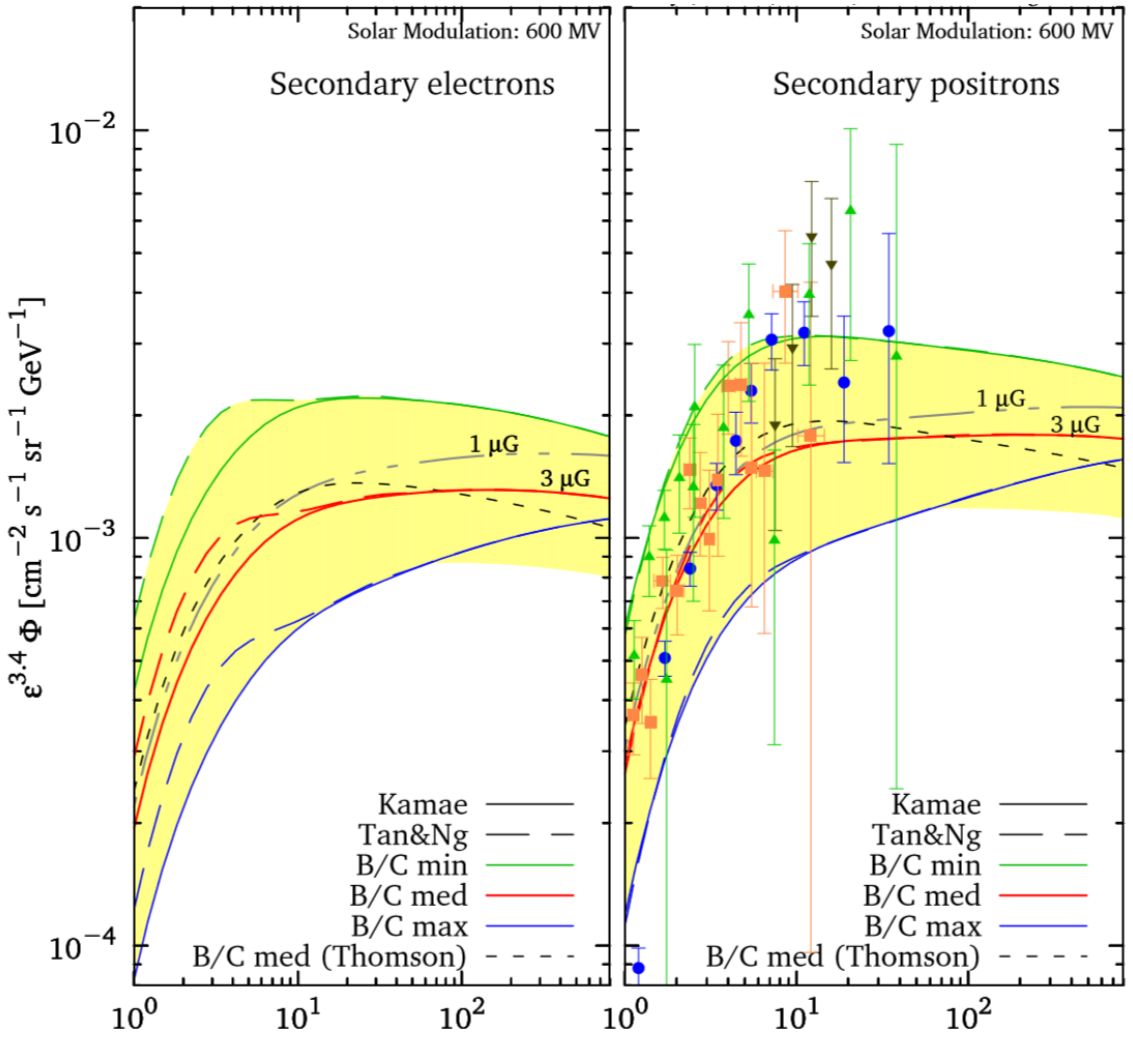

Time-dependent propagation

- For E > 80GeV, the SNRs sources are not smoothly distributed.
- The Green function is given by

$$\mathcal{G}_t(t, E, \boldsymbol{x} \leftarrow t_s, E_s, \boldsymbol{x}_s) = \delta(\Delta t - \Delta\tau)\, \mathcal{G}(E, \boldsymbol{x} \leftarrow E_s, \boldsymbol{x}_s)$$

- With $\Delta t = t - t_s$ and $\Delta\tau(E, E_s) \equiv \int_E^{E_s} \frac{dE'}{b(E')}$
- For a point source that is not far and not old

$$\phi_\odot(E) = \frac{\beta\, c}{4\pi}\, \frac{b(E^\star)}{b(E)}\, \frac{Q_{\star,0}\, \epsilon_\star^{-\gamma}}{(\pi\lambda^2)^{3/2}} \simeq \frac{c}{4\pi}\, \frac{Q_{\star,0}\, \epsilon^{-\widetilde{\gamma}_\star}}{(4\,\pi\, K_0\, t_\star)^{3/2}}$$

$$\widetilde{\gamma}_\star = \gamma + \frac{3}{2}\delta$$

Discussion of the uncertainties for a single source spectrum

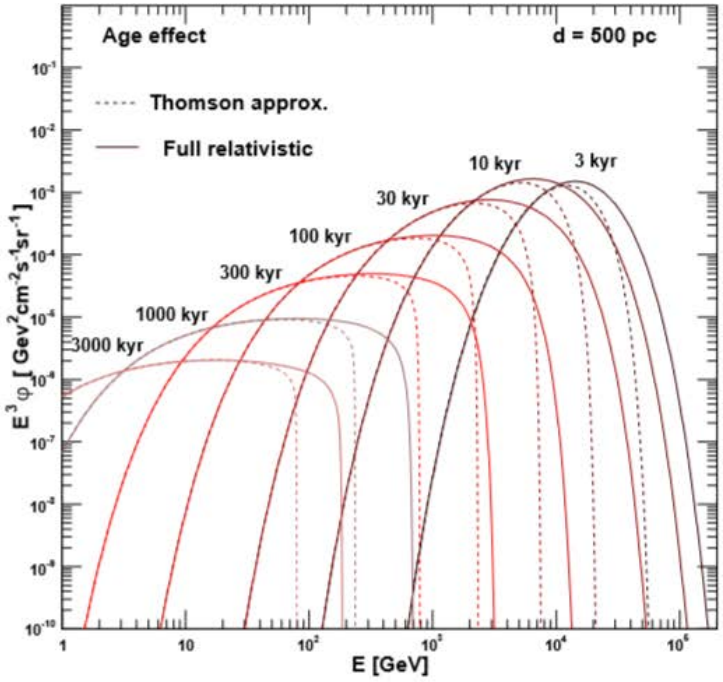

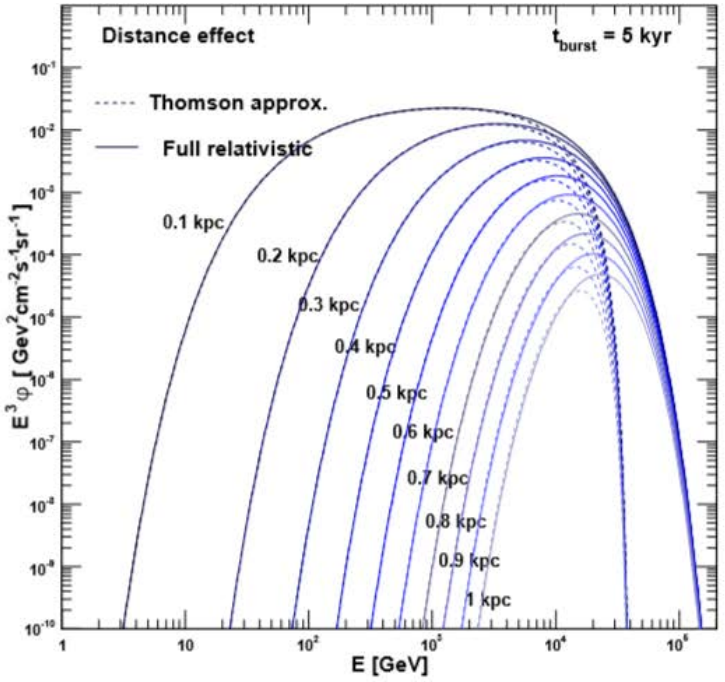

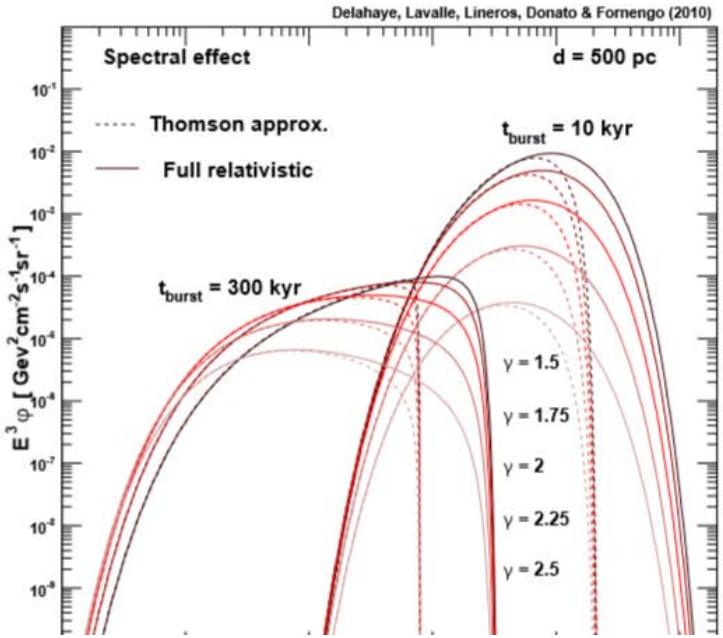

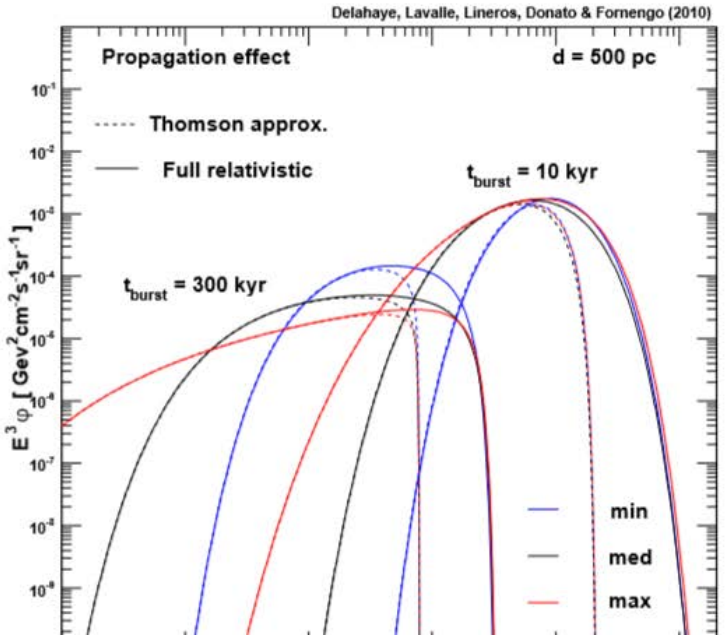

Solar modulation

• When cosmic rays enter our Solar System, they must overcome the outward-flowing solar wind. This wind impedes and slows the incoming cosmic rays, reducing their energy and preventing the lowest energy ones from reaching the Earth. This effect is known as solar modulation.

• The Sun has an 11-year activity cycle which is reflected in the ability of the solar wind to modulate cosmic rays. As a result, the cosmic ray intensity at Earth is anti-correlated with the level of solar activity, i.e., when solar activity is high and there are lots of sunspots, the cosmic ray intensity at Earth is low, and vice versa.

Modulation of Galactic Cosmic Rays Observed at the Earth
with two solar activity proxies

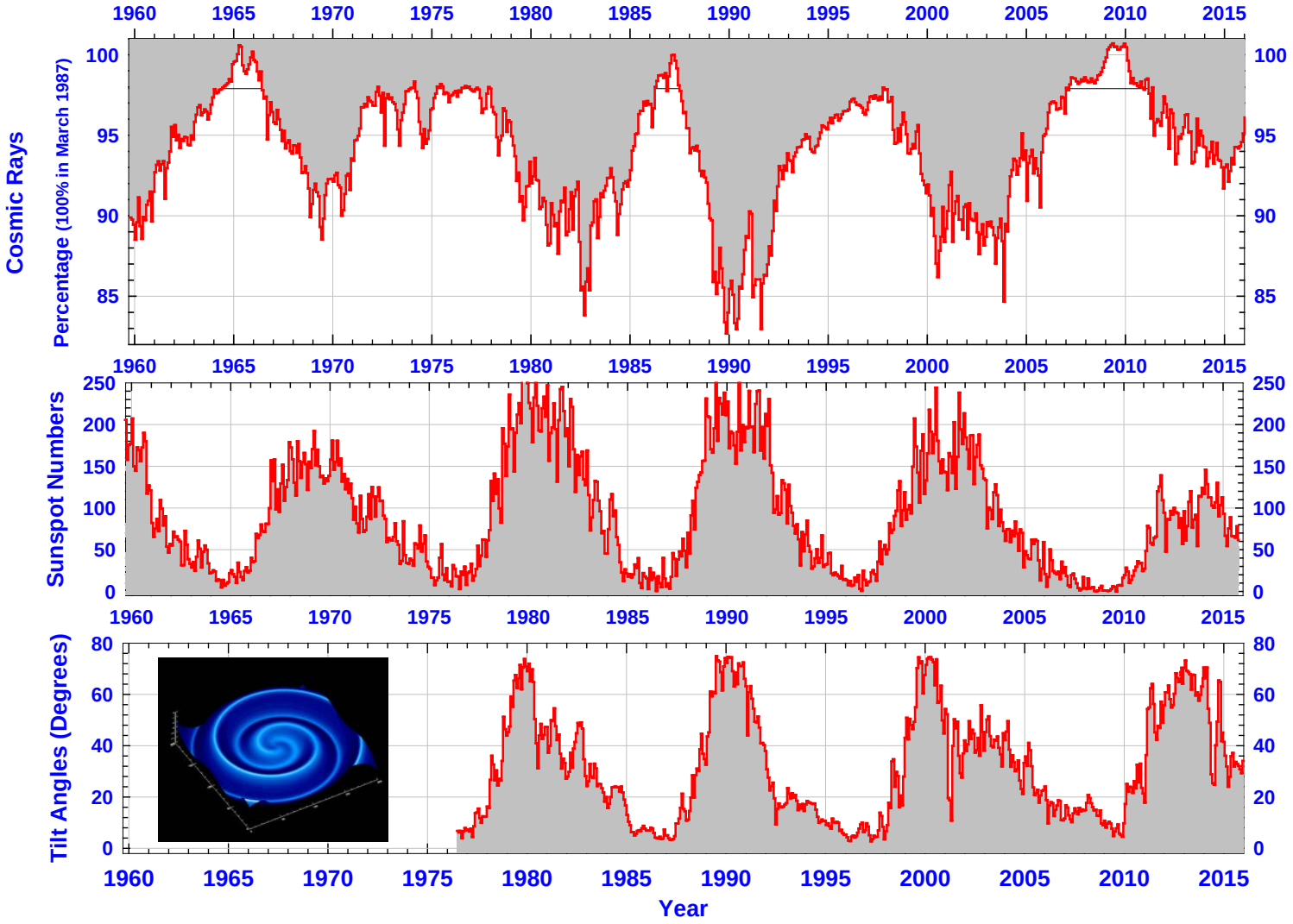

PAMELA Electron Observations and Modeling

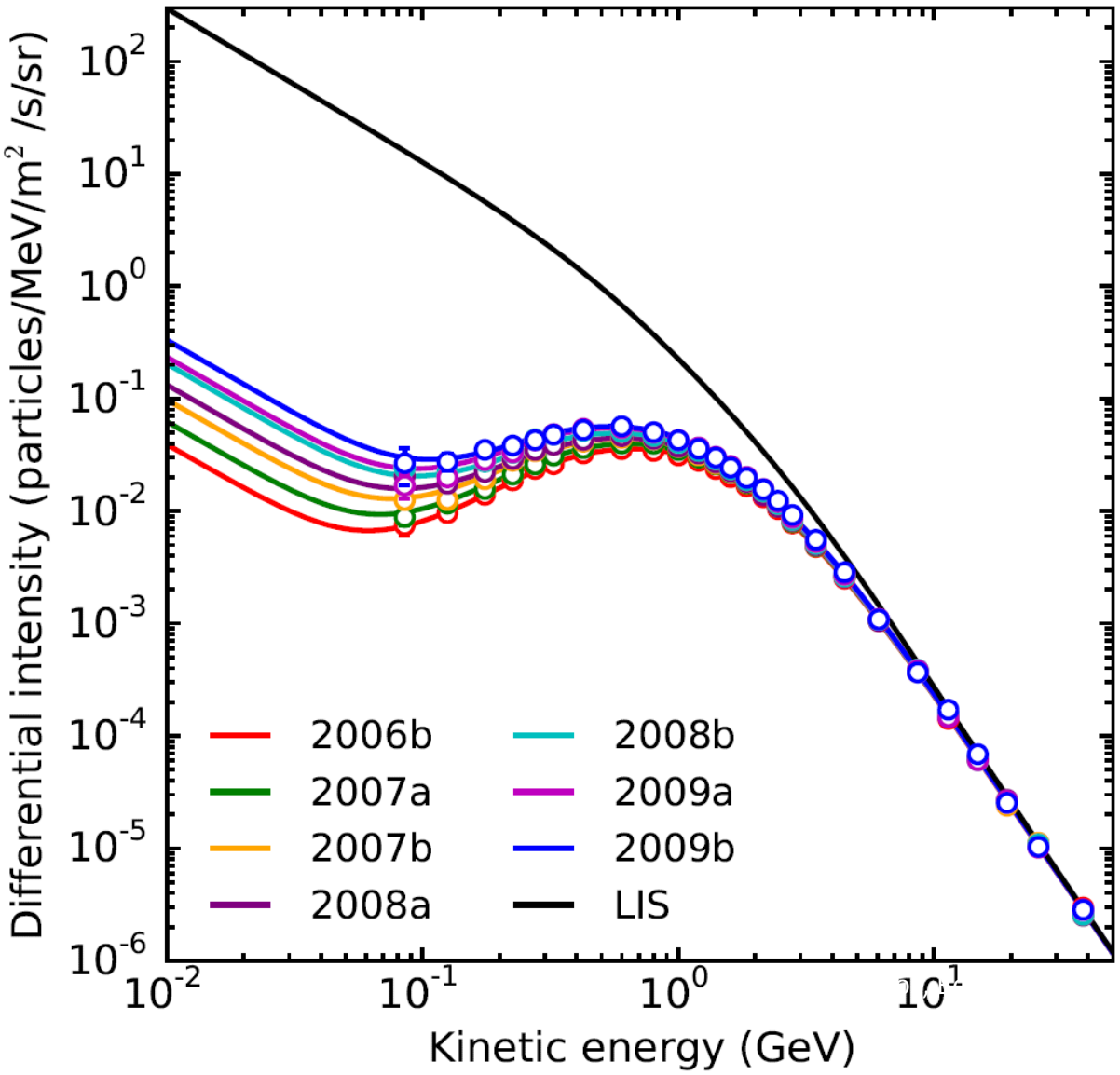

Difference between proton, electron and positron modulation

At the Earth from 2006 to 2009

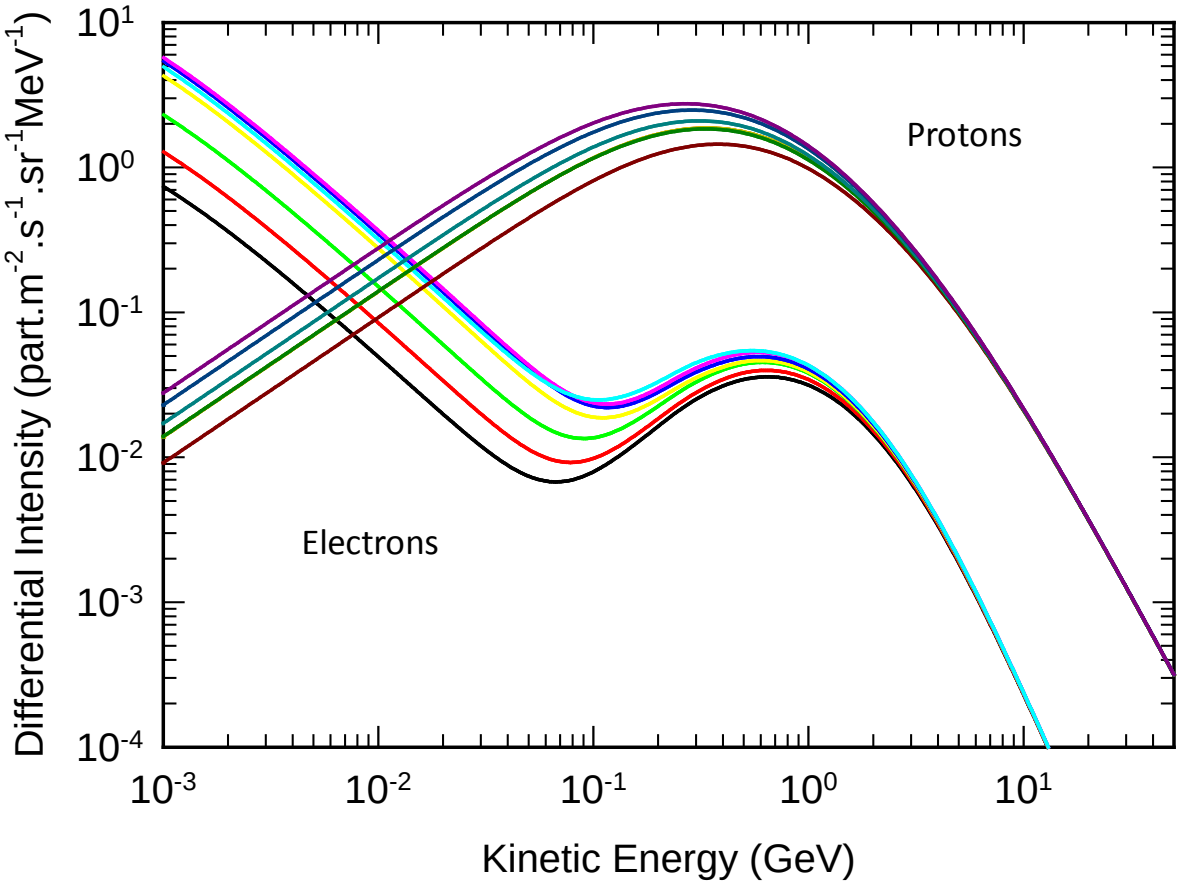

Solar modulation on charged CRs

Gleeson & Axford通过求解宇宙线在太阳磁场以及太阳风粒子作用下的传 播方程，给出宇宙线粒子流强和本地星际空间流强的关系为

$$J(E) = \frac{E^2 - m^2}{(E + |Z|\Phi)^2 - m^2} \times J_{\mathrm{LIS}}(E + |Z|\Phi),$$

其中E, m和Z分别为宇宙线粒子总能量，质量和电荷，Φ是描述调制程度的参数，和太阳活动呈正相关性。这个结果从图像上来说相当于外流的太阳风形成一个势为Φ的有效力场，宇宙线粒子进入太阳系到达地球需要克服力场做功，从而导致宇宙线粒子动能减少，减少的量等于|Z|Φ。因此该模型也被称作“力场近似”。

Oxygen cosmic ray intensity during three different periods: Sept. 1997 (squares),
Feb 2000 (circles), Jan. 2001 (diamonds)